Title

A comparative analysis between two flax varieties indicates lignan-mediated salt stress adaptiveness

Running title

Lignan-mediated salt stress adaptiveness in flax

Authors

Anirban Jyoti Debnath[1] (Corresponding author) (anirbandebnath@ymail.com) (ORCID ID: 0000-0003-1907-837X)

Ľubomír Harenčár[1] (harencar.l@gmail.com) (ORCID ID: 0000-0002-2372-6539)

Matúš Kučka[1] (mat.kucka@gmail.com) (ORCID ID: 0000-0003-1219-3519)

Marek Kovár[1] (marek.kovar@uniag.sk) (ORCID ID: 0000-0002-1478-8383)

Eva Ivanišová[2] (eva.ivanisova@uniag.sk) (ORCID ID: 0000-0001-5193-2957)

Veronika Mistríková[3] (veronika.mistrikova@savba.sk) (ORCID ID: 0000-0003-4268-6189)

Ján Gažo[1] (jan.gazo@uniag.sk) (ORCID ID: 0000-0002-8528-9223)

Katarína Ražná[1] (katarina.razna@uniag.sk) (ORCID ID: 0000-0003-2121-131X)

Addresses of authors

[1] Institute of Plant and Environmental Sciences,
Faculty of Agrobiology and Food Resources,
Slovak University of Agriculture in Nitra,
Trieda Andreja Hlinku 2,
949 76 Nitra, Slovakia

[2] Institute of Food Sciences,
Faculty of Biotechnology and Food Sciences,
Slovak University of Agriculture in Nitra,
Trieda Andreja Hlinku 2,
949 76 Nitra, Slovakia

[3] Institute of Plant Genetics and Biotechnology,
Plant Science and Biodiversity Centre,
Slovak Academy of Sciences,
P.O.Box 39 A, Akademická 2
950 07 Nitra, Slovakia

Submission Date: 12 October 2024
Number of Tables: One
Number of Figures: Eight
Word Count: 6,674 (from the start of the introduction to the start of the acknowledgements, excluding materials and methods)
Supplementary Data:
Supplementary Protocol: One
Supplementary Tables: Two

Highlight

A comparative morphological, biochemical, and genomic analysis of one-week NaCl-stressed flax varieties having contrasting lignan contents indicated the involvement of lignans in salt stress mitigation.

Abstract

United Nations' predicted forthcoming food scarcity creates an urgency in research to assess and improve agriculturally important plant yield under environmental stress conditions. In this context, lignans are potential defensive substances that accumulate in plants during abiotic stresses. Flax (*Linum usitatissimum* L.) is one of the richest lignan source. Plant genotypes differ in lignan contents. Therefore, to draw a correlation between genotype-specific lignan content and plant salinity-adaptiveness, we compared two flax varieties Flanders and Astella, where Flanders has higher lignan contents than Astella. We used a 1-week NaCl stress for the study. Post-stress morphological analyses revealed comparatively higher growth arrest in Flanders, suggesting its energy and resource-saving behaviour than Astella. Salinity-mediated reactive oxygen species production and associated cell damage were relatively greater in Astella than in Flanders. In biochemical stress marker assays, we found comparatively upregulated antioxidants and osmoprotection machinery in Flanders, showing its higher ROS scavenging and cellular protection capabilities than Astella. Moreover, the two-tailed qPCR assay showed comparatively higher upregulation of three lignan biosynthesis-related miRNAs - miR168a, miR399g, and miR828a in stressed Flanders indicating its emphasised involvement of lignans in salt stress mitigation. The results depict the superiority of Flanders in salt stress mitigation over Astella.

Keywords: Biochemical analysis, flax, lignan, miRNA, morphological analysis, salinity stress, salt stress mitigation, two-tailed qPCR assay

Abbreviations

APX = Ascorbate peroxidase

CAE = Caffeic acid

CAT = Catalase

DPPH = 2,2-Diphenyl-1-picrylhydrazyl

DMRT = Duncan's multiple range test

FDA = Fluorescein diacetate

GAE = Gallic acid

GPOX = Guaiacol peroxidase

LN = Leaf Number

LRWC = Leaf relative water content

MDA = Malondialdehyde

MYB = Myeloblastosis

PA = Phenolic acids

PCA = Principal component analysis

PCC = Pearson's correlation coefficient

PI = Propidium iodide

PP = Polyphenols

RD = Root diameter

RDW = Root dry weight

RF = Root fork

RFW = Root fresh weight

RL = Root length

RMD = Root mass density

ROS = Reactive oxygen species

RRWC = Root Relative water contents

RT = Root tip

RV = Root volume

SDW = Shoot dry weight

SFW = Shoot fresh weights

SECO = Secoisolariciresinol

SFW = Shoot fresh weight

SL = Shoot length

SOD = Superoxide dismutase

SRWC = Shoot Relative water contents

TEAC = 6-hydroxy-2,5,7,8-tetramethylchroman-2-carboxylic acid

TF = Transcription factor

TT-PCR = Two-tailed qPCR

INTRODUCTION

The rapid climatic change-mediated abiotic stresses cause the annual loss of 51–82% of crop yield in world agriculture (Onyekachi *et al.*, 2019; Oshunsanya *et al.*, 2019). Salinity, one of the major abiotic stresses, is a soil condition denoted by a high concentration of soluble salts. Soils are considered saline when the ECe is 4 dS/m or more, that is equivalent to approximately 40 mM of NaCl and generates an osmotic pressure of approximately 0.2 MPa (Munns and Tester, 2008). Presently, salinity affects around 20% of total cultivated and 33% of irrigated lands including more than 424 million hectares of topsoil (0-30 cm) and 833 million hectares of subsoil (30-100 cm) spanning 73% of the global land area (FAO, 2021). Around 195.1 million, 6.1 million, 6.73 million and 70 thousand hectares of soil are salinity-affected in Asia and the Pacific and Australia, Europe, India and Slovakia, respectively (Tractor Junction, 2022; FAO, 2023a; Stehlo and Ková, 2023). Soil salinity reduces around 1.5 million hectares of farmland annually (FAO, 2023b). By 2050, around 50% of total arable land may be affected by salinity (FAO, 2021). This alarming situation demands research to produce salinity-stress-resilient crops (UN, 2024).

High concentration of salts in soil limits a plant's water and nutrient uptake capability creating a physiologic drought condition. To balance this soil solute potential to favour stable water flux, plants channelise photosynthates in synthesising and accumulating osmolytes or compatible solutes such as proline and glycine betaine (Türkan and Demiral, 2009). The diversion of cellular resources from the major physiologic process such as photosynthesis results in drastic growth rate reduction of a salinity-affected plant. Growth arrest under stress is considered a plant adaptive mechanism to preserve carbohydrates for sustained metabolism, prolonged energy supply and better recovery after stress relief (Bartels and Sunkar, 2005).

Salinity stress disrupts the cellular balance between energy absorption and consumption. Consequently, electrons start leaking from electron transport chains of photosynthesis (chloroplast), respiration (mitochondria), and photorespiration (peroxisomes). These leaked electrons oxidise oxygen molecules creating a large amount of reactive oxygen species (ROS) that damages molecular and cellular components by oxidation of biomolecules (lipids, carbohydrates, proteins, enzymes and DNA) and cause plant death (Hasanuzzaman *et al.*, 2019; Alaei *et al.*, 2020; Mekawy *et al.*, 2020; Sachdev *et al.*, 2021). To combat this fatal situation, plant cells have a well-established ROS-scavenging antioxidant defence mechanism consisting of enzymatic components such as superoxide dismutase (SOD), catalase (CAT), ascorbate peroxidase (APX), monodehydroascorbate reductase (MDHAR), dehydroascorbate reductase (DHAR), glutathione reductase (GR), glutathione S-transferase (GST), glutathione peroxidase (GPX) and guaiacol peroxidase (GPOX) along with non-enzymatic components such as ascorbic acid (AsA), dehydroascorbate (DHA), Glutathione (GSH), alkaloids, α-tocopherol, tocotrienols, carotenoids, polyphenols, quercetin, kaempferol-glycosides, cytochromes, polyamines, proteins carrying redox-active S-groups (thioredoxins, peroxiredoxins and sulfiredoxins) and non-protein amino acids like proline (Smirnoff and Cumbes, 1989; Abogadallah, 2010; Gill and Tuteja, 2010; Hasanuzzaman *et al.*, 2019). Multiple hydroxyl groups also make polyphenols (phenolic acids, flavonoids, stilbenoids and lignans) powerful ROS scavengers (Šamec *et al.*, 2021).

Lignans are secondary metabolites belonging to the group of dimeric phenylpropanoids which naturally occur in superior plants where they primarily act in plant defence. Phenylpropanoids are phenylpropane derivatives whose skeleton consists of a propane moiety (a three-carbon chain) attached to a phenyl group. Phenylpropanoid dimers where two phenylpropane units are linked by their carbon 8 (β-β' link) represent the simplest lignan. Naturally occurring plant lignans have varying degrees of substitution in the phenylpropane skeletons (Sainvitu *et al.,* 2012; Teponno *et al.,* 2016; Markulin *et al.,* 2019; Ražná *et al.,* 2021). Lignans are found in the majority of plants. They are present in different plant organs such as flowers, seeds, leaves, roots, fruits, and wooden parts (Ražná *et al.,* 2021).

Lignans are involved in plant defence mechanisms through their antioxidant activity (Ghotbzadeh Kermani *et al.,* 2019). Synthesis of several polyphenols including lignans increases during abiotic stresses such as drought, extreme temperatures, salinity, heavy metal, and UV radiations (Sharma *et al.,* 2019; Ražná *et al.,* 2021). Under drought stress, lignan contents of sesame change in a genotype-specific manner. Moreover, the drought-tolerant sesame genotypes contain a high level of lignans such as sesamin and/or sesamolin (Ghotbzadeh Kermani *et al.,* 2019). Heavy metal stress-tolerant rapeseed (*Brassica napus* L.) genotypes accumulated more lignans under the stress of Cadmium heavy metal than the susceptible genotypes (Mwamba *et al.,* 2020). Lignans also possess antibacterial (Cespedes *et al.,* 2006; Gaafar *et al.,* 2013; Mahendra Kumar and Singh, 2015), antifungal (Cespedes *et al.,* 2006; Akiyama *et al.,* 2007; Cho *et al.,* 2007) and antifeedant (Kraus and Spiteller, 1997) properties.

MicroRNAs (miRNAs) are a class of non-coding, 19-24 nucleotide long RNA molecules that negatively regulate gene expression at the post-transcriptional level. In plants, a miRNA is loaded into the RNA-induced silencing complex (RISC) that involves argonaute (AGO) protein. The miRNA-RISC complex then binds to its target mRNA and degrades it using AGO, thereby repressing the associated gene expression (Li *et al.,* 2018). Reinhart *et al.,* (2002) detected the first-ever miRNA in plants. Besides regulating numerous physiological processes, miRNAs also impact plants' tolerance toward various abiotic stresses including salinity stress. Several miRNAs such as miR156, miR159, miR160, miR164, miR166, miR167, miR168, miR169, miR172, miR319, miR394, miR395, miR396, miR397, miR399 and miR408 are considered as conserved for salt stress in plants (Gao *et al.,* 2022). Studies depict that miRNAs impact salt stress tolerance by regulating either hormonal pathways (Sunkar *et al.,* 2012; Baek *et al.,* 2016; Liu *et al.,* 2019; Makkar *et al.,* 2021) or antioxidant systems of a plant (Noman *et al.,* 2017; Yang and Guo, 2018; Parmar *et al.,* 2020; Cheng *et al.,* 2021).

Several secondary metabolites of plants, including lignans, are biosynthesised via the phenylpropanoid pathway. Several miRNAs regulate this pathway by targeting either biosynthesis-related genes, transcription factors (TFs) or noncoding RNAs (ncRNAs) (Ražná *et al.,* 2021). In a recent study, Tu *et al.,* (2022) depicted that 23 miRNAs regulate 80 genes of the phenylpropanoid pathway belonging to 14 gene families of *Liriodendron chinense*. This study revealed the direct involvement of many novel miRNAs in this regulation process besides some of the known miRNAs such as lch-miR165a-5p, lch-miR168a-5p, lch-miR169a-3p and lch-miR393a-5p. The authors also found indirect regulation of the phenylpropanoid pathway by miRNAs and long non-coding RNAs (lncRNAs). They target

some key myeloblastosis (MYB) TFs that either act as repressors (MYB4, MYB39, MYB44 and MYB308) or activators (MYB2, MYB5, MYB12, MYB330 and MYB340) of this pathway. Phenylalanine ammonia lyase (PAL) performs the first and committed step of the phenylpropanoid pathway converting phenylalanine to cinnamic acid. Few studies reveal the involvement of miR172, miR399, miR408, miR477, miR830, miR7729 and miR1873 regulating PAL (Singh *et al.,* 2016; Yan *et al.,* 2019). In this regard, Biswas *et al.,* (2016) reported that miR172i, a member of miR172 family, regulates 4-coumarate-CoA ligase that catalyses subsequent steps of phenylpropanoid pathway of converting 4-coumarate and other 4-hydroxycinnamates to their corresponding thiol esters. Several members of the cytochromes P450 gene superfamily exert important steps in the phenylpropanoid pathway such as cinnamic acid 4-hydroxylase (C4H; CYP73A), coumarate 3-hydroxylase (C3H; CYP98A) and ferulic acid 5-hydroxylase (F5H; CYP84A) (Reinprecht *et al.,* 2017). In tea, both miR5251 and miR7777-5P.1 downregulate C4H (Sun *et al.,* 2017). A miR319-based artificial miRNA (AMR) downregulates both C3H and F5H genes in jute (Shafrin *et al.,* 2015). Barvkar *et al.,* (2013) reported that lus-miR168b regulates CYP450 genes in flax. Dimerization of monolignols to pinoresinol by the joint action of a dirigent protein (DIR) and a laccase is an important step of lignan biosynthesis (Zoclanclounon *et al.,* 2022). Three abiotic stress-responsive Indica rice miRNAs, ath-mirf10317-akr, cre-mir910, and osa-mirf10761-akr regulate DIR expression (Singh *et al.,* 2020). Cotton miRNA396 targets a dirigent-like protein (Zhang *et al.,* 2007). Multiple studies report that both miR397 and miR408 are involved in laccase gene regulation in different plants including flax (Le Roy *et al.,* 2017; Carrió-Seguí *et al.,* 2019; Li *et al.,* 2019; Ražná *et al.,* 2022; Guo *et al.,* 2023). Further downstream of the lignan biosynthesis pathway, UDP-glycosyltransferases (UGTs) glycosylate secoisolariciresinol (SECO) into secoisolariciresinol diglucoside (SDG), which is a lignan. A recent article reports a 41 miRNAs-derived regulation of 74 CsUGT genes in cucumber (Yuan *et al.,* 2024).

Being a food, oilseed and fibre crop, flax (*Linum usitatissimum*, family *Linaceae*), commonly known as flaxseed or linseed, is considered a multipurpose crop. Flaxseed is one of the richest sources of lignans. Major lignans found in flax are secoisolariciresinol diglucoside (294-2410 mg/100 gm), secoisolariciresinol (257.6 mg/ 100 gm), lariciresinol (3.04-11.46 mg/100 gm), matairesinol (0.55-6.68 mg/100 gm) and pinoresinol (3.32 mg/100 gm) (Goyal *et al.,* 2014; Rodríguez-García *et al.,* 2019). Flax is susceptible to multiple abiotic stresses such as drought, salinity and heat that endanger the plant's life and reduce its overall productivity (Yadav *et al.,* 2022). Being both a great reservoir of lignans and susceptible to salinity stress, we choose flax as the ideal study plant to draw a correlation between these two factors.

Lignans accumulate in plants and primarily act as defence substances during abiotic stresses. However, the lignan contents are dependent on plant genotypes. Therefore, we searched for the answer to the question – "under salinity stress, how much better can a high lignan-containing flaxseed genotype adapt than a low lignan-containing flaxseed genotype?". Various morphological, biochemical, microscopic, and genomic expression assays were applied to determine the salinity stress-responsiveness between the two chosen flaxseed genotypes, Flanders and Astella, having contrasting lignan content. To our knowledge, this is the first report on lignan-related miRNA-mediated salt stress tolerance study for the multi-utilitarian crop flax.

MATERIALS AND METHODS

Plant materials and salt treatment

Seeds of flax cv. Flanders and Astella were kindly provided by Agritec Plant Research Ltd., Šumperk, Czech Republic. According to the estimation of Agritec Plant Research Ltd, the lignan (Secoisolariciresinol, SECO) content of Flanders (3144.9 mg/kg) is much higher than Astella (1352.0 mg/kg). Healthy and uniform seeds were placed on tap water-moistened filter paper and incubated in a growth chamber (Climatic Chamber KK 400, Pol-Eko-Aparatura, Poland) at 23±2°C in the dark for germination. One-week-old, healthy seedlings having uniform height were transferred to TS2 white peat potting substrate (Klasmann-Deilmann GMBH, Germany) and kept in square pots (8 cm x 8 cm x 9.5 cm, length x breadth x height). Every pot had 5 seedlings. These pots were incubated in a growth chamber (Climatic Chamber KK 1200, Pol-Eko-Aparatura, Poland) at 23±2°C under a 16/8 hours photoperiod having a light intensity of 5000 lux using fluorescent tube lights and 50% humidity. The substrate was irrigated thrice a week (Monday, Wednesday, and Friday) with a watering solution (Grandiol Universal Liquid Plant Food, ASB Grünland Helmut Aurenz GmbH, Germany, 1:20 v/v dilution with distilled water) to a reference weight (pot + substrate + watering solution) of 272 grams that represented 80% of the maximum soil water-holding capacity (MSWC) of the substrate measured gravimetrically (Junker *et al.,* 2015). The seedlings were allowed to grow for two weeks more.

Experimental treatments were arranged in a randomised complete block design. A 100 mM NaCl (Sigma-Aldrich Chemie GmbH, Germany) solution prepared in distilled water was used for salt stress application. Three-week-old, randomly selected plants of both genotypes were subjected to salinity stress treatment using the NaCl solution. The watering solution was used for control treatment. The substrate was irrigated thrice (Monday, Wednesday, and Friday) to its 80% MSWC for both treatments. After one week of stress treatment (next Monday), fresh plant samples were harvested for morphological and microscopic analyses, and the rest of the samples were stored at -50°C for biochemical and genomic analysis.

Morphological assays

Various shoot, root, and leaf parameters were recorded in this assay. Due to the differential growth rates of Flanders and Astella, we processed the data in two steps to obtain an unbiased result as suggested previously (Julkowska and Testerink, 2015). Firstly, we estimated the relative changes by subtracting the values obtained before stress from values obtained after stress until otherwise mentioned. Secondly, the data were normalised against the control treatments. We plotted the normalised relative data into graphs. The percentage (%) change of salt stress treatment data was calculated against the respective controls.

Shoot length (SL) was measured using a ruler scale. Root length (RL), diameter (RD), volume (RV), and tip (RT) and fork (RF) numbers were measured using an Epson Expression 11000XL scanner coupled with WinRHIZO Pro 2013e software (Regent Instruments Inc., Canada). The scanner was calibrated for Regent Instruments Software. The RL/SL values were calculated. Relative change of leaf number (LN) under salt stress was also counted.

Shoot and root fresh weights (SFW and RFW) were measured separately using a digital balance (Explorer Analytical, Ohaus Corporation, USA). For the dry weight (SDW and RDW) measurement, freshly harvested shoot and root samples of plants were dried in Venticell LSIS-B2V/VC55 (MMM Group, USA) drying oven at 105°C for one hour and at 80°C for another four hours; weights were measured afterwards using the digital balance. Relative water contents of shoot (SRWC) and root (RRWC) were calculated according to Yan *et al.,* (2023) using the following formula:

$$\text{SRWC or RRWC} = [(FW - DW) / FW] \times 100\%$$

The RFW/SFW, RDW/SDW, and RRWC/SRWC values were calculated. Root mass density (RMD) was calculated by dividing root FW by its volume.

Leaf relative water content (LRWC) was measured according to Turner (1986). The first fifteen leaves of a plant were removed using a fine-tipped scissor and fresh weight (FW) was recorded and floated on distilled water at 4°C. After 24 hours, leaf turgid weight (TW) was recorded. The leaves were dried using the abovementioned drying procedure and dry weight (DW) was recorded. LRWC was calculated using the following formula:

$$LRWC = [(FW - DW) / (TW - DW)] \times 100\%$$

Reactive Oxygen Species (ROS) generation assay

Hydrogen peroxide (H_2O_2) concentration was determined according to Sinha (1972) to assess the extent of reactive oxygen species (ROS) generation. A mixture of 1 g of leaf sample, 100 mg activated charcoal and 10 ml 5% trichloroacetic acid (TCA) was centrifuged at 12000 rpm for 10 min. The supernatant (0.5 ml) was mixed with 0.01 M phosphate buffer, pH 7.0 to make 1 ml volume and a 3 ml mixture of potassium dichromate and glacial acetic acid (1:3 v/v) was added. The absorbance was quantified spectrophotometrically at 570 nm and the H_2O_2 concentration was estimated against standards of 10-160 μmoles.

Lipid peroxidation assays

Malondialdehyde (MDA) assay was used as a membrane lipid peroxidation marker under salt stress-derived oxidative stress damage. MDA contents were measured using thiobarbituric (TBA) method according to Dhindsa *et al.,* (1981). Briefly, a mixture of 0.1 g of leaf sample, 0.5% of TBA and 20% of trichloroacetic acid was heated in a hot water bath at 90°C for 30 min and then cooled in an ice bath. The supernatant was then extracted by centrifuging at 12000 rpm for 20 min. The absorbance for MDA was estimated at 532 nm spectrophotometrically and MDA contents were calculated using an extinction coefficient of 155/mM/cm.

Enzymatic antioxidants analyses

Sample preparation

Freshly harvested leaves were homogenised in 0.1 M potassium phosphate buffer, pH 7.8 in cold conditions. The homogenates were centrifuged at 4°C, 12000 rpm (Hettich, Germany) for 20 min. The supernatant obtained was stored at −80 °C to analyse the enzymatic activities.

SOD

SOD activity was measured based on the protocol of Giannopolitis and Ries (1977). The 3.7 ml reaction mixture contained 100 ml plant supernatant sample, 0.5 mM nitroblue tetrazolium (NBT), 17 mM methionine, 0.1 mM EDTA, 60 μm riboflavin, 0.1 M potassium phosphate buffer, pH 7.8. The one unit of SOD activity was defined as the quantity of enzyme required to inhibit photolytic reduction of nitroblue tetrazolium (NBT) by 50 %.

CAT

CAT activity was assayed by the Aebi (1984) method. The 1 ml reaction mixture contained 20 μl plant supernatant sample, 10 mM H_2O_2, and 0.05 M potassium phosphate buffer, pH 7.0. The decomposition of H_2O_2 by catalase is recorded by the decrease in absorbance per unit time at 240 nm.

APX

The Nakano and Asada (1987) method was used to estimate APX activity. The 1 ml reaction mixture contained 100 ml plant supernatant sample, 1.5 mM H_2O_2, 0.5 mM ascorbic acid, 0.1 mM EDTA, and 0.05 M potassium phosphate buffer, pH 7.0. The enzyme activity was measured by the rate of oxidation of ascorbic acid, which is directly followed by the decrease in absorbance at 290 nm per minute.

GPOX

GPOX activity was measured according to Pütter (1974). The reaction mixture contained 100 μl plant supernatant sample, 50 μl guaiacol solution, 30 μl H_2O_2, and 3 ml phosphate buffer, pH 7.0. The increase in absorbance was read at 436 nm, and GPOX activity was calculated using an extinction coefficient of 6.39 $cm^2/\mu mol$.

Non-enzymatic antioxidants analyses

Sample preparation

A 0.10 g sample was extracted with 10 ml of 80% ethanol for 2 hours. After centrifugation at 4000 g (Rotofix 32 A, Hettich, Germany) for 10 min, the supernatant was used for the following experiments.

Total polyphenol content

Total polyphenol content was measured according to Singleton and Rossi (1965) using the Folin-Ciocalteu reagent. A 0.1 ml sample was mixed with 0.1 mL of the Folin-Ciocalteu reagent, 1 mL of 20% (w/v) sodium carbonate and 8.8 ml of distilled water, and left in darkness for 30 min. The absorbance at 700 nm was measured spectrophotometrically. Gallic acid (GAE) (25-300 mg/l; R^2=0.998) was used as a standard and the results were expressed in mg/l of gallic acid equivalent. Analysis was carried out in triplicate.

Total phenolic acid content

Total phenolic acid content was determined using the method of Jain *et al.,* (2017). A 0.5 ml of sample extract was mixed with 0.5 ml of 0.5 M hydrochloric acid, 0.5 ml Arnova reagent (10% $NaNO_2$ +10% Na_2MoO_4), 0.5 ml of 1 M sodium hydroxide (w/v) and 0.5 ml of water. Absorbance at 490 nm was measured spectrophotometrically. Caffeic acid (CAE) (1 – 200 mg/l, R^2 = 0.999) was used as a standard and the results were expressed in mg/g caffeic acid equivalents. Analysis was carried out in triplicate.

Radical scavenging activity

The radical scavenging activity of samples was measured using 2,2-diphenyl-1-picrylhydrazyl (DPPH) (Sanchéz-Moreno *et al.,* 1998). The sample (0.4 ml) was mixed with 3.6 ml DPPH solution (0.025 g DPPH in 100 ml ethanol). The absorbance of the reaction mixture was determined spectrophotometrically at 515 nm. Trolox (6-hydroxy-2,5,7,8-tetramethylchroman-2-carboxylic acid; TEAC) (10-100 mg/l; R^2=0.989) was used as the standard and the results were expressed in mg/g Trolox equivalents. Analysis was carried out in triplicate.

All the chemicals used in non-enzymatic antioxidants analyses were analytical grade and purchased from Sigma-Aldrich (St. Louis, MO, USA) and CentralChem (Bratislava, Slovak Republic). The analyses were carried out in triplicate. The absorbances were measured using a Jenway spectrophotometer (6405 UV/Vis, England).

Proline content analysis

The proline content (μg/g FW of tissue) was determined by the procedure of Bates *et al.,* (1973). Leaf tissues were homogenised in sulphosalicylic acid (3% w/v) and reacted with an equal volume of acid ninhydrin and glacial acetic acid for an hour at 95 °C in a water bath. The reaction mixture was further transferred to an ice bath to terminate the reaction. After

10 min, toluene was added to each tube, shaken, and the proline concentration was estimated spectrophotometrically by measuring the absorbance at 520 nm.

RNA isolation

Total RNA was isolated from 100 mg of shoot sample using the NucleoSpin RNA Plant mini kit (Macherey-Nagel, Germany) following the kit-specified protocol. The isolated RNA was eluted in 50 µL kit-supplied RNase-free water. The quantity and purity of total RNA were estimated in NanoPhotometer P 360 (Implen GmbH, Germany) spectrophotometer.

Two-tailed qPCR (TT-PCR) assay

Expression analysis of miRNA genes was performed using the Two-Tailed qPCR Assay kit (BioVendor – Laboratorni medicina a.s., Czech Republic) following the kit-specified protocol. The relevant briefing of the TT-PCR assay protocol is provided in Supplementary Protocol S1. The protocol of the kit is biphasic. Primer sets for three miRNA genes, miR168a, miR399g and miR828a for both phases were supplied with the kit. In the first phase, cDNA was synthesised from total RNA using the C1000 thermal cycler with a dual 48/48 fast reaction module (Bio-Rad, USA). An equal volume of total RNA (326 ng) was used in all the reactions. In the second phase, qPCR was performed using the C1000 thermal cycler with CFX96 Real-Time System optical reaction module (Bio-Rad, USA). Expression of Cyclophilin and ETIF5A was used to normalise the miRNA expression levels. The specificity of qPCR products was determined based on melting curve (Cq) analysis using CFX Maestro 2.0 version 5.0.021.0616 (Bio-Rad, USA). The data was processed according to Livak and Schmittgen (2001) and expressed as fold change.

Viability assay of flax roots

The viability of flax root cells was determined by co-staining with fluorescein diacetate (FDA; Thermo Fisher Scientific) and propidium iodide (PI; Sigma Aldrich) according to a protocol of Jones et al (2016) with a few modifications. PI as a membrane-impermeable stain was used to visualise dead cells (red fluorescence) and FDA for viable cells (green fluorescence). To prepare stock solutions, five milligrams of FDA and one mg of PI were dissolved in one ml of acetone and one ml of distilled water, respectively, and stored at -20°C. The working staining solution was freshly prepared by dissolving four µl of FDA stock and ten µl of PI stock in distilled water and the volume was made up to one ml. Root samples were dipped in the stained solution and incubated for five minutes in the dark. Samples were observed using a Leica DM5500B fluorescence microscope equipped with a Leica DFC450 C digital camera (Leica Microsystems). The Leica filter set L5 (BP 480/40, DM 505, BP 527/30) was used to detect FDA staining and the N2.1 filter set (BP 515-560, DM 580, LP 590) was used for PI. The images were acquired with the LAS version 4.6 software (Leica Microsystems) and processed with the ImageJ version 1.54d software (Schneider *et al.*, 2012).

Statistical analysis

All the experiments had three biological and three technical replicates. Data were analysed by one-way analysis of variance (ANOVA) to calculate statistical significance. The significant differences in treatment data (mean ± standard error) were estimated through Duncan's multiple range test (DMRT) at $p < 0.05$ level (Duncan, 1955). Both analyses were done in SPSS version 19 (IBM Corporation, USA). Graphs were prepared in OriginPro 2021 version 9.8.0.200 (OriginLab Corporation, Northampton, MA, USA). Pearson's correlation coefficient analysis (PCC) and principal component analysis (PCA) were carried out using only the independent variables in R version 4.4.1 (R Core Team, 2024) coupled RStudio version 2024.04.2 Build 764 (Posit Team, 2024) software.

RESULTS

Effect of salinity stress on plant morphology

Our applied 100 mM salt stress using NaCl was not lethal to both the genotypes of flax. However, their differential response to salt stress was evident from both visual (Fig. 1D.1, D.2) and several morphological assessment perspectives (Fig. 1 A-C and E-I, Table 1, Supplementary Table S1). Due to the differential growth pattern of the two genotypes, we normalised all the data against control and on a relative scale against the treatment period.

Salt stress arrested the shoot growth of both cultivars. The relative shoot length (SL) of Flanders (-20.79%) was more reduced than Astella (-18.87%). The relative root length (RL) of Flanders (-20.12%) was also significantly shortened than Astella (71.81%) ($p < 0.05$) (Fig. 1A; Supplementary Table S1). The RL/SL ratio indicated that the root grew much faster than the shoot of Astella (2.12) as compared to Flanders (1.01) (Table 1). The stunted visual appearance of stressed Flanders plants among the other treatment plants corroborated the findings (Fig. 1D.1, D.2). Salinity stress affected the overall root morphology. Regardless of the treatments, the roots of both genotypes became thinner with plant age. On the one hand, the reduction of stress-mediated relative root diameter (RD) of Flanders (-6.76%) was lesser than Astella (-156.94%) (Fig. 1A; Supplementary Table S1). On the other hand, stress decreased the relative root volume (RV) of Flanders (-81.06%) higher than Astella (-29.55%) (Fig. 1B; Supplementary Table S1). As a result, the Flanders root system became significantly thicker but less voluminous than Astella ($p < 0.05$). The root relative tip (RT) and fork (RF) numbers indicate root branching (RB) status. Salt stress reduced Flanders' RT (-73.30%) and RF (-27.06%). Although the RT of Astella increased (42.80%) under stress, RF decreased (-7.5%). Comparatively with Astella, reduced RTs and RFs of Flanders depicted a lesser branched root system architecture (RSA) under stress (Fig. 1C; Supplementary Table S1). Salinity stress affected the plant biomass of both genotypes. Relative fresh weights of both shoots (SFW) and roots (RFW) of Flanders decreased (-38.94% and -17.67%, respectively) less than Astella (-57.30% and -42.78%, respectively) upon salt treatment (Fig. 1H; Supplementary Table S1). The equal RFW/SFW ratio of Flanders (1.35) and Astella (1.35) indicated an equal change of SFW and RFW in both genotypes (Table 1). Dry weights of both shoots (SDW) and roots (RDW) of Flanders (-19.06% and -46.34%, respectively) and Astella (-28.81% and -53.85%, respectively) also decreased under stress (Fig. 1H; Supplementary Table S1). However, a higher RDW/SDW ratio of Flanders (1.16) indicated a rapid RDW change than Astella (1.02) (Table 1). Shoot relative water content (SRWC) increased in Flander (2.93%) and decreased in Astella (-0.65%) under stress. Salt stress increased root relative water contents (RRWC) in Flanders (3.47%) and Astella (2.38%). However, neither of the RWCs changed significantly ($p < 0.05$) (Fig. 1F; Supplementary Table S1). The nearly equal RRWC/SRWC ratio of Flanders (1.01) and Astella (1.03) represented a similar water content change in both shoots and roots in the two genotypes (Table 1). Interestingly, leaf relative water content (LRWC), a vital marker of salt stress, was increased in Flanders (5.23%) and decreased in Astella (-7.07%). Nevertheless, the LRWC of Flanders was significantly higher than Astella ($p < 0.05$) (Fig. 1G; Supplementary Table S1). Moreover, after the stress period, the number of leaves (LN) of Astella decreased significantly (-45.31%) than that of Flanders (-1.90%), whose LN did not change significantly from the control ($p < 0.05$) (Fig. 1E; Supplementary Table S1). The results indicate that although plants of both genotypes can retain similar amounts of water in their below- and above-ground parts,

Flanders can store more water in its leaves than Astella. Salt stress increased root mass density (RMD) in Flanders dramatically (493.45%), but it was decreased in Astella (-17.01%). The change was significant between these genotypes ($p < 0.05$) (Fig. 1I; Supplementary Table S1).

We carried out fifteen morphological tests. Among them, the relative changes of Flanders were nonsignificant against the control in ten experiments (RL, RD, SFW, RFW, SDW, RDW, LN, SRWC, RRWC and LRWC) as compared to seven experiments for Astella (SL, SDW, RD, RF, SRWC, RRWC and LRWC) ($p < 0.05$). The data shows that Flanders' morphological responses are less affected than Astella under 100 mM NaCl stress.

Effect of salinity stress on ROS generation and cell damage

The cellular extent of salt stress-derived ROS generation and subsequent damage can be estimated by H_2O_2 and lipid peroxidation assays, respectively. Salt stress increased the H_2O_2 level in Astella (661.71%) considerably more than in Flanders (256.17%) (Fig. 2A; Supplementary Table S2). MDA is the final product of lipid peroxidation and is widely considered an oxidative stress-mediated cell membrane damage indicator. MDA content in Astella (457.03%) was higher than in Flanders (270.73%) (Fig. 2B; Supplementary Table S2). Both changes were significant against their respective controls and between genotypes ($p < 0.05$). The results suggest that Astella was experiencing more salt toxicity than Flanders.

Effect of salinity stress on antioxidant system

We found several enzymatic and non-enzymatic antioxidant markers were hyperactivated in Flanders and Astella upon NaCl stress treatment. However, the stress-mediated responses were genotype-dependent.

SOD, CAT, APX and GPOX are important cellular markers of enzymatic antioxidant systems. Moderate activation of SOD was found in both genotypes under stress. The SOD activity of stress-treated Flanders (0178.29%) increased higher than Astella (121.83%) (Fig. 3A; Supplementary Table S2). NaCl stress hyperactivated CAT in all treatment plants. A remarkable increase of CAT activity was found in stressed Flanders (1178.78%) than in Astella (609.27) (Fig. 3B; Supplementary Table S2). Stress-mediated APX activation was moderately higher in Flanders (183.11%) than in Astella (139.74%) (Fig. 3C; Supplementary Table S2). A dramatically increased GPOX activity was found in stress-treated Flanders (352.54%) which was also higher than Astella (224.20) (Fig. 3D; Supplementary Table S2). Enzyme activity changes were significantly higher in the treatment plants than in their respective control plants in all the experiments; the changes were also significant between the treatments of the two genotypes ($p < 0.05$).

Polyphenols (PP) and phenolic acids (PA) are vital non-enzymatic antioxidant system markers. NaCl stress elevated the PP contents of Flanders (35.70%) but lowered in Astella (-37.10%) (Fig. 4A; Supplementary Table S2). Also, the PA content change of Flanders (9.41%) was contrasting to Astella (-48.62%) upon saline treatment (Fig. 4B; Supplementary Table S2). The DPPH assay measures the total radical scavenging activity of antioxidants in a cell. We found that the radical scavenging activity increased in Flanders (32.36%) and

decreased in Astella (-41.90%) under salt stress (Fig. 4C; Supplementary Table S2). One of the vital components of the cellular stress mitigation system is proline which contributes to osmoregulation and antioxidant activity. Treatment plants of both genotypes had a remarkably higher proline accumulation against the respective controls. However, Flanders (9.91 ± 0.16 μMol/g FW) had an elevated proline content than Astella (6.59 ± 0.15 μMol/g FW) under stress (Fig. 4D; Supplementary Table S2). All these changes were significant between treatment and their respective control and between the treatments of two genotypes ($p < 0.05$).

All these biochemical tests to assess antioxidant activity revealed that the antioxidant system of both genotypes was heightened under stress. The salt stress-mediated antioxidant hyperactivity of Flanders than Astella was also notable.

Effect of salinity stress Lignan-related miRNAs

In this experiment, we monitored the expression of three miRNA molecules, miR168a, miR399g, and miR828a using the two-tailed qPCR (TT-PCR) assay. We found that all these molecules were upregulated under NaCl stress in both genotypes.

The miR168a was upregulated in Flanders (8.31-fold) than in Astella (3.24-fold) upon stress treatment (Fig. 5A). The Flanders gene was significantly upregulated against its control and stress-treated Astella. However, the upregulation in treated Astella was non-significant against control ($p < 0.05$). We observed the upregulation of miR399a was 13.01-fold and 6.53-fold in salt-treated Flanders and Astella, respectively (Fig. 5B). But these changes were non-significant ($p < 0.05$). The expression of miR828a was significantly upregulated in Flanders (5.84-fold) under stress. We noted that the salt stress-mediated upregulated of Astella (3.11-fold) was non-significant against control (Fig. 5C). The stress-mediated miR828a expression difference between these two genotypes was also not significant ($p < 0.05$).

Effect of salt stress on roots cell viability

We observed the viability of NaCl stress-affected roots under the microscope. Alive and dead cells appeared green and red respectively, under our differential FDA-PI staining. In both genotypes, root tips (Fig. 6A, B) and lateral root buds (Fig. 6C, D) were alive; the epidermis of the rest of the roots was dead. We found a sporadic pattern of live cells in the root maturation zone (Fig. E, F). Root cross-sectional views depicted thriving root tissues despite the damaged epidermis layers (Fig. 6G, H).

Pearson's correlation coefficient and principal component analysis

Pearson's correlation coefficient (PCC) and principal component analysis (PCA) depicted that all our experiments influenced the study outcome. PCC analysis revealed that H_2O_2 was significantly correlated with proline (100%, $p < 0.001$), highly correlated with CAT (95%), APX (80%), PA (73%), miR168a (83%), miR399g (91%), and miR828a (90%), moderately correlated with MDA (54%), and negatively correlated with majority

morphological markers. MDA was moderately correlated with proline (54%), weakly correlated with antioxidants and miRNAs, and negatively correlated with majority of the morphological markers. Interestingly, PP was moderately correlated with MDA (44%) and negatively correlated with mostly rest of our studied markers (Fig. 7A). We verified the correlation analysis with PCA. It revealed PC1 and PC2 variance of 54.96% and 29.83%, respectively. CAT, miRNAs, H_2O_2, and Proline were the major positive variables in PC1. RD, LRWC, LN, and SFW were the major positive variables in PC2. Both PCC and PCA plots depicted that CAT, APX, and PA were highly correlated with miRNAs in this study (Fig. 7B).

DISCUSSION

Multiple abiotic stresses, including salinity stress, reduce the productivity of the lignan-rich muti-utilitarian crop flax (Goyal *et al.,* 2014; Yadav *et al.,* 2022). Flax salt tolerance has been assessed in many studies (X. Li *et al.,* 2022; Y. Li *et al.,* 2022; Siddiqui *et al.,* 2022; Wang *et al.,* 2022; Hussein, 2023; Yaşar, 2023; Bayram *et al.,* 2024; Yadav, 2024). Lignans have been reported to be useful in abiotic stress mitigation in other plants except flax (Paniagua *et al.,* 2017; Ghotbzadeh Kermani *et al.,* 2019; Sharma *et al.,* 2019; Mwamba *et al.,* 2020; Ražná *et al.,* 2021). Therefore, for the first time, we assessed the unexplored role of lignan in flax salinity stress mitigation in this study. We selected two flax varieties Flanders (SECO: 3144.9 mg/kg) and Astella (SECO: 1352.0 mg/kg) of contrasting lignan content and compared their performance under salinity stress. We applied 100 mM NaCl stress as per the previous reports of salinity stress studies on flax (Qayyum *et al.,* 2019; Varga *et al.,* 2020; Hussein and Alshammari, 2022; X. Li *et al.,* 2022; Wang *et al.,* 2022; Zeki Koçak *et al.,* 2022). We carried out our experiments 21-d post-germination of flax plants because flax undergoes a transition of slower to faster growth at this age (Y. Li *et al.,* 2022). Salinity initiates two stresses in plants – osmotic and ionic. The osmotic stress mostly affects plant morphology. In ionic stress, physiologic ion and nutrient homeostasis imbalance leads to oxidative stress-mediated cell damage (Munns and Tester, 2008). We assayed various morphological and biochemical markers to understand the effect of these two phases. Additionally, we carried out genomic and microscopic assays to comprehend the study in detail.

Salinity stress caused more growth arrest in Flanders than in Astella

Plant roots are the first organ to perceive salinity stress. In saline conditions, less soil water and nutrient availability create physiologic drought in plants, initiating osmotic stress. Plants respond immediately with growth reduction in this phase affecting aerial parts too (Munns and Tester, 2008). Our morphological analyses revealed stress-derived growth arrest through lower relative SL and several root traits such as RD, RV, and RF from the control in both flax genotypes (Fig. 1A, B; Supplementary Table S1). Such growth arrest is thought to occur via gene expression reprogramming and altered hormonal homeostasis of plants under osmotic stress that decreases cell division, cell elongation, and meristem size and activity (West *et al.,* 2005; Bartels and Sunkar, 2005). Interestingly, the RL and RT of Astella were increased from control by salinity treatment. Such a contradictory observation has already been reported and explains the genotype-specificity of stress tolerance (Robin *et al.,* 2016; Saddiq *et al.,* 2021). In our study, significantly lower RL, RD, RV, and RB in Flanders represented a comparatively better RSA development in Astella under stress. Previously reported salinity stress-derived hindrance of lateral root primordia formation (McLoughlin *et al.,* 2012) could potentially explain the lower RB of our Flanders. The arrested growth of stressed Flanders can also be visually observed (Fig. 1D.1, D.2). Such growth attenuation under saline conditions has been commonly observed in other plants (Ma *et al.,* 2010; Li *et al.,* 2013; Zeeshan *et al.,* 2020; Colaneri *et al.,* 2014; Lu *et al.,* 2023) including flax (Mekawy *et al.,* 2020; X. Li *et al.,* 2022; Y. Li *et al.,* 2022; Wang *et al.,* 2022).

Along with the visual morphology of flax plants, biomass is also altered under salinity stress in our study. We observed a remarkable reduction of stress-mediated relative SFW,

SDW, RFW, and RDW in both genotypes, although the changes were not statistically different among Flanders and Astella (Fig. 1H; Supplementary Table S1). The physiologic drought and cellular nutritional imbalance-derived oxidative stress damage vital photosynthetic enzymes leads to reduced photosynthesis in a salinity-affected plant (Munns, 2002; Ueda *et al.,* 2003; Mekawy *et al.,* 2020; Yildiz *et al.,* 2020; Zhao *et al.,* 2021). Photosynthesis impairment results in drastic growth rate reduction-derived low plant biomass (De Herralde *et al.,* 1998; Bartels and Sunkar, 2005). However, in this critical condition, higher ratios of RL/SL, RFW/SFW, and RDW/SDW in our salt-treated flax plants represented better survival of roots than shoots in saline conditions (Table 1). The equal RFW/SFW ratio of Flanders and Astella evidenced their indifferent root-shoot growth rate under stress. However, Contrasting RL/SL and RDW/SDW ratios represented despite having a smaller RSA, Flanders can equally maintain its shoots biomass compared to Astella. It indicated a better stress management approach for Flanders than Astella. Continuation of root growth under salt stress appears to facilitate water uptake from deeper soil layers and removes toxic ions from the plant's body, leading to lower physiologic salt concentration (Bartels and Sunkar, 2005; Acosta-Motos *et al.,* 2017), report also exists where smaller RSA facilitated shoot growth under stress (Ma *et al.,* 2010). Our results are consistent with previous findings (Sengupta and Majumder, 2009; Hu *et al.,* 2012; Wang *et al.,* 2020, 2022;).

Moreover, salt stress inhibits leaf initiation possibly by suppressing leaf primordia (Dolatabadian *et al.,* 2011; Farooq *et al.,* 2015). We also found relative LN reduction upon stress treatment (Fig. 1E; Supplementary Table S1) that possibly contributed to further photosynthesis reduction on a whole plant level. The statistically non-significant minuscule reduction of stressed Flanders relative LN from control stated that new leaf initiation was not much affected under stress in this genotype. On the contrary, the significantly higher relative LN of Flanders indicated a comparatively lower progressive damage rate and better health of leaf initiation mechanism than Astella during the stress period as reported previously (Yildrim *et al.,* 2008; Rahneshan *et al.,* 2018; Dikobe *et al.,* 2021).

Relative water contents are important plant traits for salinity stress assessment (Tao *et al.,* 2021; Ahmed *et al.,* 2022). We found an increase and decrease of LRWC in salt-treated Flanders and Astella, respectively from their controls. The LRWC of Flanders was significantly higher than that of Astella. We also observed a statistically non-significant change of SRWC and RRWC in all treatments of the two genotypes (Fig 1f, g; Supplementary Table S1). It signifies that despite the similar water content of below- and above-ground plant parts, the leaf of Flanders was holding more water than Astella under stress. Higher LRWC often signifies better salinity stress management in various plants (Rodríguez *et al.,* 2005; Esringü *et al.,* 2005; Boussora *et al.,* 2024) including flax (Siddiqui *et al.,* 2022; Y. Li *et al.,* 2022), indicating better salt stress management of Flanders than Astella in our study.

Tissue density is a functional plant trait associated with growth and survival (Birouste *et al.,* 2014). It correlates positively with growth rate (Ryser and Lambers, 1995; Poorter and De Jong, 1999). The drastic upregulation of RMD in Flanders supports its slower growth rate than Astella under stress (Fig. 1I, Supplementary Table S1). Our findings agree with previous reports (Louw-Gaume *et al.,* 2010; Tang, 2019).

The results depicted that under stress, Flanders was restricting shoot and root growth more, retaining more leaf water, and having denser root mass than Astella. In practice, Flanders was arresting its growth and saving vital resources under stress. This is a well-known stress-adaptive phenomenon.

Salinity stress was causing more harm to Astella

We found a significant increase in ROS (expressed by H_2O_2) and lipid peroxidation (expressed by MDA) in salt-stressed Flanders and Astella. (Fig. 2A, B; Supplementary Table S2). The production of ROS molecules such as superoxide ($O_2^{\bullet-}$), hydroxyl ($^{\bullet}OH$), alkoxyl ($RO^{\bullet}$) and peroxyl ($ROO^{\bullet}$) radicals, hydrogen peroxide (H_2O_2), singlet oxygen ($^1O_2$), and ozone (O_3) are natural byproducts of normal cellular metabolic processes. Plant cells generally maintain a dynamic balance of ROS and ROS-scavenging antioxidants to achieve a neutral redox potential state (Hasanuzzaman *et al.,* 2019; Sachdev *et al.,* 2021). The balance alters when salinity stress overwhelms the antioxidant defence and causes electron leakage by disrupting the electron flow in photosynthesis, photorespiration, and electron transport chain apparatuses. These leaked electrons partially reduce O_2 and trigger ROS. It initiates the so-called cellular "oxidative burst". The most dangerous outcome of oxidative stress is ROS-mediated lipid peroxidation which generates MDA. Lipid peroxidation destroys cell membranes causing cell death (Ahmad *et al.,* 2008; Gill and Tuteja, 2010). H_2O_2 and MDA have been considered important stress markers in many previous studies with flax (Alaei *et al.,* 2020; Kiani *et al.,* 2020; Hussein and Alshammari, 2022; Siddiqui *et al.,* 2022; Wang *et al.,* 2022). Elevated ROS and lipid peroxidation are reported to be associated with salt susceptibility compared to a tolerant variety in many plants such as rice (Chawla *et al.,* 2013; Kaur *et al.,* 2016), *Brassica juncea* (Kumar *et al.,* 2018), wheat and barley (Zeeshan *et al.,* 2020; Ashraf *et al.,* 2023) and safflower (Vijayalakshmi *et al.,* 2016). In our study, the significantly higher ROS and MDA levels in Astella signified its greater ROS-mediated cell damage and lower salt tolerance than in Flanders. It also indicated the existence of a comparatively better ROS scavenging system in Flander compared to Astella that minimises ROS and associated cell damage.

Salinity stress hyperactivated the antioxidant system in Flanders

Plants activate the antioxidant defence system to mitigate oxidative stress. In our study, enzymatic antioxidants (SOD, CAT, APX, and GPOX) were upregulated upon salt stress in both genotypes (Fig. 3A-D; Supplementary Table S2). Comparatively, Flanders's antioxidant system was significantly upregulated over Astella after stress application. SOD gives frontline defence against ROS by dismuting $O_2^{\bullet-}$ to H_2O_2 (Gill and Tuteja, 2010). H_2O_2 is quickly scavenged by CAT, GPOX, and APX and converted to H_2O and O_2 (Carrasco-Ríos and Pinto, 2014; Hasanuzzaman *et al.,* 2019; Mekawy *et al.,* 2020). In plants, H_2O_2 has a dual role – 1) at low concentrations, it acts as a signalling molecule to activate various pathways to alleviate stress; 2) at high concentrations, it acts as a toxic substance and initiates programmed cell death (PCD) (Saxena *et al.,* 2016). In our study, the comparatively lower concentration of H_2O_2 in Flanders possibly hyperactivates its antioxidant system than in Astella under stress.

Various non-enzymatic antioxidants are also excellent ROS scavengers in plants. PP and one of its sub-categories PA are important plant stress markers (Šamec *et al.,* 2021). We found PP and PA were upregulated in Flanders and downregulated in Astella under stress (Fig. 4A, B; Supplementary Table S2). Salt stress influences the levels of various PP compounds by affecting key enzyme activities of their centralised biosynthesis using the phenylpropanoid pathway (Sharma *et al.,* 2019). According to the previous reports, PP (Kiani *et al.,* 2021; Lungoci *et al.,* 2022; Sarker *et al.,* 2023) and PA (Singh *et al.,* 2013; Ozfidan-Konakci *et al.,* 2015) contents generally increase under salt stress. However, opposite reports do exist. Slama *et al.,* (2017) reported declining PP content at elevated salt concentrations in *Sesuvium portulacastrum*. Total PP content decreased after salt treatment in both salt-sensitive and -tolerant genotypes of Medicago (Salah *et al.,* 2011). In Romaine lettuce, despite the total PP content increase, PA content decreased after 100 mM NaCl stress (Mahmoudi *et al.,* 2010). Telesiński *et al.,* (2008) found that the total PP content of bean plants decreased and enzymatic antioxidants increased under salt stress; according to them, stress-derived nutrient deprivation was the main culprit for antioxidant hypoactivation. In our study, ROS-mediated photosynthetic apparatus damage and a decrease in overall photosynthesis level due to low LN could result in the decline of non-enzymatic antioxidant contents in Astella over control under salt stress. Moreover, ROS-derived damage of antioxidant biosynthetic pathway enzymes (Dunn, 1998) could have accelerated the injury. Lower radical scavenging activity of Astella than its control could also be correlated with enzyme damage (Fig. 4C; Supplementary Table S2).

Multiple studies compared salt sensitivity between known tolerant and susceptible genotypes and established the connection between elevated antioxidant activity and salinity stress tolerance in plants (Neto *et al.,* 2006; Chutipaijit *et al.,* 2005; Aktas, 2012; Chawla *et al.,* 2013; Vijayalakshmi *et al.,* 2016; Kaur *et al.,* 2016; Kumar *et al.,* 2018; Wang *et al.,* 2019). We also found significant upregulations in various antioxidant components and radical scavenging activity between Flanders and Astella under stress. It signified a better antioxidant system-mediated superior salinity resilience of Flanders than Astella.

Proline was providing multi-dynamic protection to Flanders

We found remarkable upregulations of proline in both genotypes under stress (Fig. 4D; Supplementary Table S2). Proline has multifaceted roles in salt stress mitigation by – 1) acting as an osmolyte and helping to stabilise the disrupted osmoregulation in salinity-affected cells; 2) scavenging ROS molecules; 3) maintaining Na^+, K^+, Ca^+, and Cl^- homeostasis in affected cells; 4) restoring redox homeostasis of injured cells; 5) providing energy during nutrient deprivation; 6) maintaining metabolic balance by crosslinking multiple pathways; 7) upregulating antioxidant synthesis; 8) acting as chaperon to protect antioxidant enzymes (Smirnoff and Cumbes, 1989; Cuin and Shabala, 2007; Kaul *et al.,* 2008; Liang *et al.,* 2013; Kaur and Asthir, 2015; Mansour and Ali, 2017; Truong *et al.,* 2023). Due to the wide array of stress-adaptive functions, proline is generally upregulated during abiotic stresses and is considered a crucial salinity stress index (Mansour and Ali, 2017). Salt treatment-mediated proline upregulation in tolerant genotypes has already been reported in different plants (Kumar *et al.,* 2018; Nguyen *et al.,* 2021; Vasilakoglou *et al.,* 2021) including flax (Y. Li *et al.,* 2022). Therefore, the comparatively increased proline accumulation in

stressed Flanders further supported its better salt stress mitigation capability than Astella. Moreover, lower proline accumulation in stressed Astella signified its lesser degree of protection against salt stress and could also explain its elevated ROS level and decreased antioxidant activity under stress.

Lignan-related miRNAs were upregulated under salt stress

We analysed the expressions of three lignan biosynthesis-related miRNAs - miR168a, miR399g, and miR828a, using a kit-based two-tailed qPCR (TT-PCR) assay. Originally designed by Androvic *et al.,* (2017), very few reports of the TT-PCR assay to measure plant microRNA expression exist to date (Anna *et al.,* 2019; Barczak-Brzyżek *et al.,* 2022; Kong *et al.,* 2022; Pawełkowicz *et al.,* 2022). We are reporting a kit-based two-tailed qPCR (TT-PCR) assay for the first time. Our tested miRNAs were upregulated in both genotypes under salt stress (Fig. 5A-C).

The miR168 family containing miR168a and miR168b is well-known to express under salt stress in various plants (Li *et al.,* 2012; Xia *et al.,* 2023) including flax (Barvkar *et al.,* 2013; Yu *et al.,* 2016). Under salt stress, miR168 primarily affects AGO1 of RISC via feedback downregulation (Ding *et al.,* 2009). Since AGO is a core component of the RISC complex that guides miRNAs to cleave complementary target-mRNAs, the downregulation could impact global miRNA action by potentially adjusting metabolic processes in response to salt stress (Carnavale Bottino *et al.,* 2013). Studies have also shown that miR168 affects the expression of CYP450 in flax (Barvkar *et al.,* 2013) and rice (Wei and Chen, 2018). CYP450 is a critical controller of the phenylpropanoid pathway that produces lignan. Therefore, under salt stress, miR168 can affect lignan biosynthesis by affecting the phenylpropanoid pathway via deregulation of CYP450 (Reinprecht *et al.,* 2017; Zhang *et al.,* 2022).

The role of miR399 plant phosphate starvation is well established; little is known about its function in salt stress. The miR399 family consists of six members, from miR399a to miR399f, each member has a different role in salt stress. Upregulation of Arabidopsis miR399f during salt treatment has been reported (Bari *et al.,* 2006; Baek *et al.,* 2016). Upon salt treatment, Lu *et al.,* (2011) observed upregulation of TAmiR399 in wheat and Lelandais-Briere (2009) observed downregulation of Mtr-miR399 in *Medicago truncatula*. Possibly these two groups observed different miR399 family members and therefore obtained contrasting results. Islam *et al.,* (2022) proposed that miR399 is involved in the ABA metabolic pathway during salt stress. In an *in-silico* analysis, Yan *et al.,* (2019) reported that ata-miR399a-5p regulates the JrPAL3 gene of the phenylpropanoid pathway of lignan biosynthesis.

Reports of miR828 involvement in salt stress are also meagre. Shuai *et al.,* (2016) reported that miR828 is expressed under abiotic stress. Under salt stress, miR828 can either directly upregulate various MYB transcription factors (TFs) (Deng and Lu 2017), or it can upregulate TAS4 family phased secondary small interfering RNAs (phasiRNAs) (Fei *et al.,* 2013; Shuai *et al.,* 2016; Liu *et al.,* 2020; Mittal *et al.,* 2023; Panchal, 2023; Xie *et al.,* 2023). The phasiRNAs can upregulate various MYB TFs (Luo *et al.,* 2012; Zhang 2015). MYB TFs

can promote lignan biosynthesis (Chiang *et al.,* 2019; Markulin *et al.,* 2019; Pratyusha and Sarada 2022; Ražná *et al.,* 2022; Xie *et al.,* 2023).

Studies related to the role of lignan-related miRNAs for salt stress mitigation are minuscule, and according to the available reports, our results connect miRNAs to lignan via some mediators. These mediators mostly affect the phenylpropanoid pathway, which produces many (secondary) metabolites, including lignan. Nevertheless, most miRNAs regulate multiple target sequences across numerous biological processes. It is a densely interconnected regulatory network and its pleiotropic effect is obvious (Wang *et al.,* 2024). Therefore, our study provides indicative, rather than direct evidence of lignan involvement in flax salt stress mitigation.

Salt stress affected root cell viability

Our FDA and PI differential staining revealed alive root tips and lateral root buds stained green. The dead epidermis of the rest of the roots was stained red (Fig. 6A-H). Roots are the primary organ of plants that are affected by salt stress (AbdElgawad *et al.,* 2016). Since soil salinity creates physiologic drought in plants, they respond similarly under drought and salt stress. Previously, Duan *et al.,* (2010) reported salt stress-mediated ROS generation damaged the root cells of the meristematic and elongation zone ceasing the overall root growth. Such stress-mediated root damage could have minimised root growth more in Flanders than in Astella in our study. Moreover, direct exposure of root epidermis cells, the outmost layer of roots, to the high soil salt concentration must have induced a high level of oxidative burst that damaged them the most.

Morphological, biochemical, and genomic markers are correlated with salt stress response

We correlated our measured variables using PCC and PCA to understand their cumulative effect on stress in this study (Fig. 7A, B). To understand the extent of salt stress-derived cellular oxidative stress and associated cell damage, we represented H_2O_2 and MDA as ROS and cell damage markers, respectively. Our tested morphological trait variables were negatively correlated with H_2O_2, MDA, antioxidants, and miRNAs. It showed that our finding of salt stress-mediated growth arrest (Fig. 1A-I) was due to the elevated ROS, cell damage, and cellular defence mechanism. The growth retarding effect of our tested miRNAs is not well studied and therefore, it needs to be investigated further.

ROS generation was positively correlated with antioxidants, proline, and miRNAs signifying their simultaneous activation under salt stress. The correlation between ROS and cell damage was moderate. The co-upregulation and salinity-ameliorate role of antioxidants and proline to minimise ROS has already been established (Hasanuzzaman *et al.,* 2019; Y. Li *et al.,* 2022) and is also reflected in our study (Fig. 3A-D, 4A-D). The strong positive correlations between our studied miRNAs with ROS supported the connection of these miRNAs with salt stress mitigation. Strong alleviation of ROS by antioxidants, proline, and miRNAs could have weakened the associated cell damage in the flax plants we studied. CAT, APX, PA and miRNAs had the strongest stress mitigation effect.

PP was positively correlated with MDA and negatively correlated with H_2O_2, signified only cell damage could trigger PP. However, PP was negatively correlated with the rest of our tested antioxidants and miRNAs. It indicated an undiscovered complex homeostatic relation between PP and the rest of our tested antioxidants and miRNAs for salt stress mitigation. Such a homeostatic relationship should be verified for its existence in further studies. Lignan is a type of PP. In our study, we found that salt stress upregulated lignan-related miRNAs (Fig. 5A-C). Therefore, we can speculate that a progressive increase in salt stress would upregulate lignans in the PP-antioxidant-miRNA homeostatic pool.

Based on the findings, we hypothesised a salt stress-adaptive model for flax (Fig. 8).

Conclusion

This paper reports the salt stress adaptive differential response of two flax cultivars, Flanders and Astella, having contrasting lignan contents. Under stress, we found arrested growth, lower ROS generation, lower cell damage, higher activities of antioxidant system components, higher amount of proline, and upregulated lignan biosynthesis-related miRNAs in Flanders over Astella. This study is the first report on kit-based TT-PCR assay. Root viability assay using differential staining depicted the existence of viable root tips despite ROS-mediated cell damage. Multivariant correlation analyses revealed the relationships of our experiments. The correlation analyses divulged a few knowledge caveats that have potential for future research. Our results established Flanders as the superior flax genotype over Astella for salt stress adaptation.

SUPPLEMENTARY DATA

The following supplementary data are available at JXB online.

Protocol S1. TT-PCR assay method briefing.

Table S1. Summary of various morphological parameter changes of two flax genotypes Flanders and Astella under 100 mM NaCl treatment.

Table S2. Summary of different biochemical parameter changes of two flax genotypes Flanders and Astella under 100 mM NaCl treatment.

ACKNOWLEDGEMENTS

We acknowledge Ing. Janka Šimková, Institute of Biodiversity and Biological Safety, Slovak University of Agriculture in Nitra for helping with plant photography.

AUTHOR CONTRIBUTIONS

AJD and KR: conceptualisation, methodology, and fellowship; AJD, ĽH, MatK, MarK, EI, and VM: investigation; AJD and JG: data curation and formal analysis; AJD: visualisation, and writing – original draft preparation; KR: funding acquisition, project administration, resources, supervision, and validation; AJD, ĽH, MatK, MarK, EI, VM, JG, KR: writing – review and editing.

CONFLICT OF INTEREST

The authors declare no conflict of interest.

FUNDING STATEMENT

This work was supported by The National Scholarship Programme of The Slovak Republic by The Ministry of Education, Science, Research and Sport, Government of The Slovak Republic (NSP-SAIA).

DATA AVAILABILITY

The raw dataset of the independent variables is available on Zenodo (https://doi.org/10.5281/zenodo.13907999) (Debnath *et al.*, 2024).

REFERENCES

AbdElgawad H, Zinta G, Hegab MM, Pandey R, Asard H, Abuelsoud W. 2016. High Salinity Induces Different Oxidative Stress and Antioxidant Responses in Maize Seedlings Organs. Frontiers in Plant Science **7**, 276.

Abogadallah GM. 2010. Insights into the significance of antioxidative defense under salt stress. Plant Signaling and Behavior **5**, 369-374.

Acosta-Motos JR, Ortuño MF, Bernal-Vicente A, Diaz-Vivancos P, Sanchez-Blanco MJ, Hernandez JA. 2017. Plant Responses to Salt Stress: Adaptive Mechanisms. Agronomy **7**, 18.

Aebi H. 1984. Catalase in vitro. Methods in Enzymology **105**, 121-126.

Ahmed HGM, Zeng Y, Raza H, Muhammad D, Iqbal M, Uzair M, Khan MA, Iqbal R, El Sabagh A. 2022. Characterization of wheat (*Triticum aestivum* L.) accessions using morpho-physiological traits under varying levels of salinity stress at seedling stage. Frontiers in Plant Science **13**, 953670.

Ahmad P, Sarwat M, Sharma S. 2008. Reactive oxygen species, antioxidants and signaling in plants. Journal of Plant Biology **51**, 167-173.

Aktas H, Abak K, Eker S. 2012. Anti-oxidative responses of salt-tolerant and salt-sensitive pepper (*Capsicum annuum* L.) genotypes grown under salt stress. The Journal of Horticultural Science and Biotechnology **87**, 360-366.

Akiyama K, Yamauchi S, Nakato T, Maruyama M, Sugahara T, Kishida T. 2007. Antifungal activity of tetra-substituted tetrahydrofuran lignan, (-)-virgatusin, and its structure-activity relationship. Bioscience, Biotechnology, and Biochemistry **71**, 1028-1035.

Alaei Y, Kazemitabar SK, Zaeifi Zadeh M, Najafi Zarini H, Kiani G. 2020. A study on the salinity stress effects on the biochemical traits of seedlings and its relationship with resistance toward sensitive and tolerant flax genotypes. Journal of Applied Biology and Biotechnology **8**, 47-52.

Androvic P, Valihrach L, Elling J, Sjoback R, Kubista M. 2017. Two-tailed RT-qPCR: a novel method for highly accurate miRNA quantification. Nucleic Acids Research **45**, e144.

Anna BB, Grzegorz B, Marek K, Piotr G, Marcin F. 2019. Exposure to High-Intensity Light Systemically Induces Micro-Transcriptomic Changes in *Arabidopsis thaliana* Roots. International Journal of Molecular Sciences **20**, 5131.

Ashraf MA, Hafeez A, Rasheed R, Hussain I, Farooq U, Rizwan M, Ali S. 2023. Evaluation of Physio-Morphological and Biochemical Responses for Salt Tolerance in Wheat (*Triticum aestivum* L.) Cultivars. Journal of Plant Growth Regulation **42**, 4402-4422.

Baek D, Chun HJ, Kang S, Shin G, Park SJ, Hong H, Kim C, Kim DH, Lee SY, Kim MC, Yun DJ. 2016. A role for Arabidopsis *miR399f* in salt, drought, and ABA signaling. Molecules and Cells **39**, 111-118.

Barczak-Brzyżek A, Brzyżek G, Koter M, Siedlecka E, Gawroński P, Filipecki M. 2022. Plastid retrograde regulation of miRNA expression in response to light stress. BMC Plant Biology **22**, 150.

Bari R, Datt Pant B, Stitt M, Scheible WR. 2006. PHO2, microRNA399, and PHR1 define a phosphate-signaling pathway in plants. Plant Physiology **141**, 988-999.

Bartels D, Sunkar R. 2005. Drought and Salt Tolerance in Plants. Critical Reviews in Plant Sciences **24**, 23-58.

Barvkar VT, Pardeshi VC, Kale SM, Qiu S, Rollins M, Datla R, Gupta VS, Kadoo NY. 2013. Genome-wide identification and characterization of microRNA genes and their targets in flax (*Linum usitatissimum*): Characterization of flax miRNA genes. Planta **237**, 1149-1161.

Bates LS, Waldren RP, Teare ID. 1973. Rapid determination of free proline for water-stress studies. Plant and Soil **39**, 205-207.

Bayram ÇŞ, Yalınkılıç AN, & Başbağ S. 2024. Investigation of Germination and Early Seedling Development of Some Flax (*Linum usitatissimum* L.) Seeds Under Salt Stress. Manas Journal of Agriculture Veterinary and Life Sciences **14**, 64-70.

Birouste M, Zamora-Ledezma E, Bossard C, Pérez-Ramos IM, Roumet C. 2014. Measurement of fine root tissue density: a comparison of three methods reveals the potential of root dry matter content. Plant and Soil **374**, 299-313.

Biswas S, Hazra S, Chattopadhyay S. 2016. Identification of conserved miRNAs and their putative target genes in *Podophyllum hexandrum* (Himalayan Mayapple) Plant Gene **6**, 82-89.

Boussora F, Triki T, Bennani L, Bagues M, Ben Ali S, Ferchichi A, Ngaz K, Guasmi F. 2024. Mineral accumulation, relative water content and gas exchange are the main physiological regulating mechanisms to cope with salt stress in barley. Scientific Reports **14**, 14931.

Carnavale Bottino M, Rosario S, Grativol C, Thiebaut F, Rojas CA, Farrineli L, Hemerly AS, Ferreira PC. 2013. High-throughput sequencing of small RNA transcriptome reveals salt stress regulated microRNAs in sugarcane. PLOS One **8**, e59423.

Carrió-Seguí À, Ruiz-Rivero O, Villamayor-Belinchón L, Puig S, Perea-García A, Peñarrubia L. 2019. The Altered Expression of *microRNA408* Influences the Arabidopsis Response to Iron Deficiency. Frontiers in Plant Science **10**, 324.

Céspedes CL, Avila JG, Garcıá AM, Becerra J, Flores C, Aqueveque P, Bittner M, Hoeneisen M, Martinez M, Silva M. 2006. Antifungal and antibacterial activities of *Araucaria araucana* (Mol.) K. Koch heartwood lignans. Zeitschrift fur Naturforschung. C, Journal of biosciences **61**, 35-43.

Chawla S, Jain S, Jain V. 2013. Salinity induced oxidative stress and antioxidant system in salt-tolerant and salt-sensitive cultivars of rice (*Oryza sativa* L.). Journal of Plant Biochemistry and Biotechnology **22**, 27-34.

Cheng XL, He Q, Tang S, Wang HR, Zhang XX, Lv MJ, Liu HF, Gao Q, Zhou Y, Wang Q, Man XY, Liu J, Huang RF, Wang H, Chen T, Liu J. 2021. The miR172/IDS1 signaling module confers salt tolerance through maintaining ROS homeostasis in cereal crops. New Phytologist **230**, 1017-1033.

Chiang NT, Wen CH, Chu FH. 2019. *TcMYB1*, *TcMYB4*, and *TcMYB8* participate in the regulation of lignan biosynthesis in *Taiwania cryptomerioides* Hayata. Tree Genetics and Genomes **15**, 67.

Cho JY, Choi GJ, Son SW, Jang KS, Lim HK, Lee SO, Sung ND, Cho KY, Kim JC. 2007. Isolation and antifungal activity of lignans from Myristica fragrans against various plant pathogenic fungi. Pest Management Science **63**, 935-940.

Chutipaijit S, Cha-Um S, Sompornpailin K. 2009. Differential accumulations of proline and flavonoids in indica rice varieties against salinity. Pakistan Journal of Botany **41**, 2497-2506.

Colaneri AC, Tunc-Ozdemir M, Huang JP, Jones AM. 2014. Growth attenuation under saline stress is mediated by the heterotrimeric G protein complex. BMC Plant Biology **14**, 129.

Cuin TA, Shabala S. 2007. Compatible solutes reduce ROS-induced potassium efflux in *Arabidopsis* roots. Plant, Cell & Environment **30**, 875-885.

De Herralde F, Biel C, Savé R, Morales MA, Torrecillas A, Alarcón JJ, Sánchez-Blanco MJ. 1998. Effect of water and salt stresses on the growth, gas exchange and water relations in *Argyranthemum coronopifolium* plants. Plant Science **139**, 9-17.

Debnath AJ, Harenčár Ľ, Kučka M, Kovár M, Ivanišová E, Mistríková V, Gažo J, Razna K. 2024. Dataset from the article "A comparative analysis between two flax varieties indicates lignan-mediated salt stress adaptiveness" [Data set]. Zenodo. doi: 10.5281/zenodo.13907999

Deng Y, Lu S. 2017. Biosynthesis and Regulation of Phenylpropanoids in Plants. Critical Reviews in Plant Sciences **36**, 257-290.

Dikobe T, Mashile B, Sinthumule R, Ruzvidzo O. 2021. Distinct Morpho-Physiological Responses of Maize to Salinity Stress. American Journal of Plant Sciences **12**, 946-959.

Ding D, Zhang L, Wang H, Liu Z, Zhang Z, Zheng Y. 2009. Differential expression of miRNAs in response to salt stress in maize roots. Annals of Botany **103**, 29-38.

Dolatabadian A, Modarres Sanavy Sam, Ghanati F. 2011. Effect of Salinity on Growth, Xylem Structure and Anatomical Characteristics of Soybean. Notulae Scientia Biologicae **3**, 41-45.

Duan Y, Zhang W, Li B, Wang Y, Li K, Sodmergen, Han C, Zhang Y, Li X. 2010. An endoplasmic reticulum response pathway mediates programmed cell death of root tip induced by water stress in Arabidopsis. New Phytologist **186**, 681-695.

Duncan DB. 1955. Multiple range and multiple F test. Biometrics **11**, 1-42.

Dunn DC, Duncan LW, Romeo JT. 1998. Changes in arginine, PAL activity and nematode behaviour in salinity-stressed citrus. Phytochemistry **49**, 413-417.

El-Beltagi HS, Salama ZA, El Hariri DM. 2008. Some biochemical Markers for Evaluation of Flax Cultivars Under Salt Stress Conditions. Journal of Natural Fibers **5**, 316-330.

Esringü A, Kant C, Yildirim E, Karlidag H, Turan M. 2011. Ameliorative Effect of Foliar Nutrient Supply on Growth, Inorganic Ions, Membrane Permeability, and Leaf Relative Water Content of Physalis Plants under Salinity Stress. Communications in Soil Science and Plant Analysis **42**, 408-423.

FAO. 2021. Global map of salt-affected soils (GSASmap v1.0). https://www.fao.org/documents/card/en/c/cb7247en Accessed October 2024

FAO. 2023a. Global Soil Partnership. https://www.fao.org/global-soil-partnership/areas-of-work/soil-salinity/en/ Accessed October 2024

FAO. 2023b. Salt-affected soils. https://www.fao.org/soils-portal/soil-management/management-of-some-problem-soils/salt-affected-soils/more-information-on-salt-affected-soils/en/ Accessed October 2024

Farooq M, Hussain M, Wakeel A, Siddique KHM. 2015. Salt stress in maize: effects, resistance mechanisms, and management. A review. Agronomy for Sustainable Development **35**, 461-481.

Gaafar AA, Salama ZA, Askar MS, El-Hariri DM, Bakry BA. 2013. In vitro antioxidant and antimicrobial activities of Lignan flax seed extract (*Linum usitatissimum*, LInternational journal of pharmaceutical sciences review and research **23**, 291-297.

Ghotbzadeh Kermani S, Saeidi G, Sabzalian MR, Gianinetti A. 2019. Drought stress influenced sesamin and sesamolin content and polyphenolic components in sesame (*Sesamum indicum* L.) populations with contrasting seed coat colors. Food Chemistry **289**, 360-368.

Giannopolitis CN, Ries SK. 1977. Superoxide dismutases: I. Occurrence in higher plants. Plant Physiology **59**, 309-314.

Gill SS, Tuteja N. 2010. Reactive oxygen species and antioxidant machinery in abiotic stress tolerance in crop plants. Plant Physiology and Biochemistry **48**, 909-930.

Goyal A, Sharma V, Upadhyay N, Gill S, Sihag M. 2014. Flax and flaxseed oil: an ancient medicine & modern functional food. Journal of Food Science and Technology **51**, 1633-1653.

Guo Y, Wang S, Yu K, Wang HL, Xu H, Song C, Zhao Y, Wen J, Fu C, Li Y, Wang S, Zhang X, Zhang Y, Cao Y, Shao F, Wang X, Deng X, Chen T, Zhao Q, Li L, Wang G, Grünhofer P, Schreiber L, Li Y, Song G, Dixon RA, Lin J. 2023. Manipulating

microRNA *miR408* enhances both biomass yield and saccharification efficiency in poplar. Nature Communications **14**, 4285.

Harshavardhan VT, Wu TM, Hong CY. 2017. Glutathione Reductase and Abiotic Stress Tolerance in Plants. In: Hossain MA, Mostofa MG, Diaz-Vivancos P, Burritt DJ, Fujita M, Tran LSP, eds. Glutathione in Plant Growth, Development, sand Stress Tolerance. Cham, Switzerland: Springer, 265-286.

Hasanuzzaman M, Bhuyan MHMB, Anee TI, Parvin K, Nahar K, Mahmud JA, Fujita M. 2019. Regulation of Ascorbate-Glutathione Pathway in Mitigating Oxidative Damage in Plants under Abiotic Stress. Antioxidants (Basel) **8**, 384.

Hu L, Huang Z, Liu S, Fu L. 2012. Growth Response and Gene Expression in Antioxidant-related Enzymes in Two Bermudagrass Genotypes Differing in Salt Tolerance. Journal of the American Society for Horticultural Science **137**, 134-143.

Hussein HA. 2023. Thiourea induces antioxidant mechanisms of salt tolerance in flax plants. Physiology and Molecular Biology of Plants. doi: 10.1007/s12298-023-01357-x

Hussein HA, Alshammari SO. 2022. Cysteine mitigates the effect of NaCl salt toxicity in flax (*Linum usitatissimum* L) plants by modulating antioxidant systems. Scientific Reports **12**, 11359.

Islam W, Waheed A, Naveed H, Zeng F. 2022. MicroRNAs Mediated Plant Responses to Salt Stress. Cells **11**, 2806.

Jain R, Rao B, Tare AB. 2017. Comparative analysis of the spectrophotometry based total phenolic acid estimation methods. Journal of Analytical Chemistry **72**, 972-976.

Jones K, Kim DW, Park JS, Khang CH. 2016. Live-cell fluorescence imaging to investigate the dynamics of plant cell death during infection by the rice blast fungus *Magnaporthe oryzae*. BMC Plant Biology **16**, 69.

Julkowska MM, Testerink C. 2015. Tuning plant signaling and growth to survive salt. Trends in Plant Science **20**, 586-594.

Junker A, Muraya MM, Weigelt-Fischer K, Arana-Ceballos F, Klukas C, Melchinger AE, Meyer RC, Riewe D, Altmann T. 2015. Optimizing experimental procedures for quantitative evaluation of crop plant performance in high throughput phenotyping systems. Frontiers in Plant Science **5**, 770.

Kaul S, Sharma SS, Mehta IK. 2008. Free radical scavenging potential of L-proline: evidence from in vitro assays. Amino Acids **34**, 315-320.

Kaur G, Asthir B. 2015. Proline: a key player in plant abiotic stress tolerance. Plant Biology **59**, 609-619.

Kaur N, Dhawan M, Sharma I, Pati PK. 2016. Interdependency of Reactive Oxygen Species generating and scavenging system in salt sensitive and salt tolerant cultivars of rice. BMC Plant Biology **16**, 131.

Kiani R, Arzani A, Mirmohammady Maibody SAM. 2021. Polyphenols, Flavonoids, and Antioxidant Activity Involved in Salt Tolerance in Wheat, *Aegilops cylindrica* and Their Amphidiploids. Frontiers in Plant Science **12**, 646221.

Kiani R, Nazeri V, Shokrpour M, Hano C. 2020. Morphological, Physiological, and Biochemical Impacts of Different Levels of Long-Term Water Deficit Stress on *Linum album* Ky. ex Boiss. Accessions. Agronomy **10**, 1966.

Kong L, Zhuo Y, Xu J, Meng X, Wang Y, Zhao W, Lai H, Chen J, Wang J. 2022. Identification of long non-coding RNAs and microRNAs involved in anther development in the tropical *Camellia oleifera*. BMC Genomics **23**, 596.

Kraus C, Spiteller G. 1997. Comparison of phenolic compounds from galls and shoots of Picea glauca. Phytochemistry **44**, 59-67.

Kumar M, Kumar R, Jain V, Jain S. 2018. Differential behavior of the antioxidant system in response to salinity induced oxidative stress in salt-tolerant and salt-sensitive cultivars of *Brassica juncea* L. Biocatalysis and Agricultural Biotechnology **13**, 12-19.

Le Roy J, Blervacq AS, Créach A, Huss B, Hawkins S, Neutelings G. 2017. Spatial regulation of monolignol biosynthesis and laccase genes control developmental and stress-related lignin in flax. BMC Plant Biology **17**, 124.

Lee RC, Feinbaum RL, Ambros V. 1993. The *C. elegans* heterochronic gene lin-4 encodes small RNAs with antisense complementarity to lin-14. Cell **75**, 843-854.

Lelandais-Brière C, Naya L, Sallet E, Calenge F, Frugier F, Hartmann C, Gouzy J, Crespi M. 2009. Genome-wide *Medicago truncatula* small RNA analysis revealed novel microRNAs and isoforms differentially regulated in roots and nodules. Plant Cell **21**, 2780-2796.

Li C, Li D, Zhou H, Li J, Lu S. 2019. Analysis of the laccase gene family and miR397-/miR408-mediated posttranscriptional regulation in *Salvia miltiorrhiza*. PeerJ **7**, e7605.

Li W, Cui X, Meng Z, Huang X, Xie Q, Wu H, Jin H, Zhang D, Liang W. 2012. Transcriptional regulation of Arabidopsis *MIR168a* and *ARGONAUTE1* homeostasis in abscisic acid and abiotic stress responses. Plant Physiology **158**, 1279-1292.

Li X, Guo D, Xue M, Li G, Yan Q, Jiang H, Liu H, Chen J, Gao Y, Duan L, Xie L. 2022a. Genome-Wide Association Study of Salt Tolerance at the Seed Germination Stage in Flax (*Linum usitatissimum* L.). Genes (Basel) **13**, 486.

Li Y, Chen J, Li X, Jiang H, Guo D, Xie F, Zhang Z, Xie L. 2022b. Adaptive Response and Transcriptomic Analysis of Flax (*Linum usitatissimum* L.) Seedlings to Salt Stress. Genes (Basel) **13**, 1904.

Li YJ, Fang Y, Fu YR, Huang JG, Wu CA, Zheng CC. 2013. NFYA1 is involved in regulation of postgermination growth arrest under salt stress in Arabidopsis. PLOS One **8**, e61289.

Li Z, Xu R, Li N. 2018. MicroRNAs from plants to animals, do they define a new messenger for communication? Nutrition & Metabolism (London) **15**, 68.

Liang X, Zhang L, Natarajan SK, Becker DF. 2013. Proline mechanisms of stress survival. Antioxidants & Redox Signaling **19**, 998-1011.

Liu Y, Teng C, Xia R, Meyers BC. 2020. PhasiRNAs in Plants: Their Biogenesis, Genic Sources, and Roles in Stress Responses, Development, and Reproduction. Plant Cell **32**, 3059-3080.

Liu YR, Li DY, Yan JP, Wang KX, Luo H, Zhang WJ. 2019. MiR319-mediated ethylene biosynthesis, signalling and salt stress response in switchgrass. Plant Biotechnology Journal **17**, 2370-2383.

Livak KJ, Schmittgen TD. 2001. Analysis of relative gene expression data using real-time quantitative PCR and the 2(-Delta Delta C(T)) Method. Methods **25**, 402-408.

Louw-Gaume AE, Rao IM, Gaume AJ, Frossard E. 2010. A comparative study on plant growth and root plasticity responses of two Brachiaria forage grasses grown in nutrient solution at low and high phosphorus supply. Plant and Soil **328**, 155-164.

Lu C, Li L, Liu X, Chen M, Wan S, Li G. 2023. Salt Stress Inhibits Photosynthesis and Destroys Chloroplast Structure by Downregulating Chloroplast Development-Related Genes in Robinia pseudoacacia Seedlings. Plants (Basel) **12**, 1283.

Lu W, Li J, Liu F, Gu J, Guo C, Xu L, Zhang H, Xiao K. 2011. Expression pattern of wheat miRNAs under salinity stress and prediction of salt-inducible miRNAs targets. Frontiers of Agriculture in China **5**, 413-422.

Lungoci C, Motrescu I, Filipov F, Jitareanu CD, Teliban G-C, Ghitau CS, Puiu I, Robu T. 2022. The Impact of Salinity Stress on Antioxidant Response and Bioactive Compounds of *Nepeta cataria* L. Agronomy **12**, 562.

Luo QJ, Mittal A, Jia F, Rock CD. 2012. An autoregulatory feedback loop involving *PAP1* and *TAS4* in response to sugars in Arabidopsis. Plant Molecular Biology **80**, 117-129.

Ma SC, Li FM, Xu BC, Huang ZB. 2010. Effect of lowering the root/shoot ratio by pruning roots on water use efficiency and grain yield of winter wheat. Field Crops Research **115**, 158-164.

Mahendra Kumar C, Singh SA. 2015. Bioactive lignans from sesame (*Sesamum indicum* L.): evaluation of their antioxidant and antibacterial effects for food applications. Journal of Food Science and Technology **52**, 2934-2941.

Mahmoudi H, Huang J, Gruber MY, Kaddour R, Lachaal M, Ouerghi Z, Hannoufa A. 2010. The impact of genotype and salinity on physiological function, secondary metabolite accumulation, and antioxidative responses in lettuce. Journal of Agricultural and Food Chemistry **58**, 5122-5130.

Makkar H, Arora S, Khuman AK, Chaudhary B. 2021. Target-mimicry-based miR167 diminution confers salt-stress tolerance during in vitro organogenesis of tobacco (*Nicotiana tabacum* L.). Journal of Plant Growth Regulation **41**, 1462-1480.

Mansour MMF, Ali EF. 2017. Evaluation of proline functions in saline conditions. Phytochemistry **140**, 52-68.

Markulin L, Corbin C, Renouard S, Drouet S, Gutierrez L, Mateljak I, Auguin D, Hano C, Fuss E, Laine E. 2019. Pinoresinol-lariciresinol reductases, key to the lignan synthesis in plants. Planta **249**, 1695-1714.

Markulin L, Drouet S, Corbin C, Decourtil C, Garros L, Renouard S, Lopez T, Mongelard G, Gutierrez L, Auguin D, Lainé E, Hano C. 2019. The control exerted by ABA on lignan biosynthesis in flax (*Linum usitatissimum* L.) is modulated by a Ca2+ signal transduction involving the calmodulin-like LuCML15b. Journal of Plant Physiology **236**, 74-87.

McLoughlin F, Galvan-Ampudia CS, Julkowska MM, Caarls L, van der Does D, Laurière C, Munnik T, Haring MA, Testerink C. 2012. The Snf1-related protein kinases SnRK2.4 and SnRK2.10 are involved in maintenance of root system architecture during salt stress. The Plant Journal **72**, 436-449.

Mekawy AMM, Assaha DVM, Ueda A. 2020. Differential Salt Sensitivity of Two Flax Cultivars Coincides with Differential Sodium Accumulation, Biosynthesis of Osmolytes and Antioxidant Enzyme Activities. Journal of Plant Growth Regulation **39**, 1119-1126.

Mittal M, Dhingra A, Dawar P, Payton P, Rock CD. 2023. The role of microRNAs in responses to drought and heat stress in peanut (*Arachis hypogaea*). Plant Genome **16**, e20350.

Munns R. 2002. Comparative physiology of salt and water stress. Plant, Cell and Environment **25**, 239-250.

Munns R, Tester M. 2008. Mechanisms of salinity tolerance. Annual Review of Plant Biology **59**, 651-681.

Mwamba TM, Islam F, Ali B, Lwalaba JLW, Gill RA, Zhang F, Farooq MA, Ali S, Ulhassan Z, Huang Q, Zhou W, Wang J. 2020. Comparative metabolomic responses of low- and high-cadmium accumulating genotypes reveal the cadmium adaptive mechanism in *Brassica napus*. Chemosphere **250**, 126308.

Nakano Y, Asada K. 1987. Purification of ascorbate peroxidase in spinach chloroplasts: its inactivation in ascorbate-depleted medium and reactivation by monodehydroascorbate radical. Plant Cell Physiology **28**, 131-140.

Neto ADA, Prisco JT, Enéas-Filho J, de Abreu CEB, Gomes-Filho E. 2006. Effect of salt stress on antioxidative enzymes and lipid peroxidation in leaves and roots of salt-tolerant and salt-sensitive maize genotypes. Environmental and Experimental Botany **56**, 87-94.

Nguyen HTT, Das Bhowmik S, Long H, Cheng Y, Mundree S, Hoang LTM. 2021. Rapid Accumulation of Proline Enhances Salinity Tolerance in Australian Wild Rice *Oryza australiensis* Domin. Plants (Basel) **10**, 2044.

Noman A, Aqeel M. 2017. miRNA-based heavy metal homeostasis and plant growth. Environmental Science and Pollution Research **24**, 10068-10082.

Onyekachi OG, Boniface OO, Gemlack NF, Nicholas N. 2019. The Effect of Climate Change on Abiotic Plant Stress: A Review. In: Bosco de Oliveira A, ed. Abiotic and Biotic Stress in Plants. London, UK: IntechOpen.

Oshunsanya SO, Nwosu NJ, Li Y. 2019. Abiotic Stress in Agricultural Crops Under Climatic Conditions. In: Jhariya MK, Banerjee A, Meena RS, Yadav DK, eds. Sustainable Agriculture, Forest and Environmental Management. Singapore: Springer, 71-100.

Ozfidan-Konakci C, Yildiztugay E, Kucukoduk M. 2015. Protective roles of exogenously applied gallic acid in *Oryza sativa* subjected to salt and osmotic stresses: effects on the total antioxidant capacity. Plant Growth Regulation **75**, 219-234.

Panchal A, Maurya J, Seni S, Singh RK, Prasad M. 2023. An insight into the roles of regulatory ncRNAs in plants: An abiotic stress and developmental perspective. Plant Physiology and Biochemistry **201**, 107823.

Paniagua C, Bilkova A, Jackson P, Dabravolski S, Riber W, Didi V, Houser J, Gigli-Bisceglia N, Wimmerova M, Budínská E, Hamann T, Hejatko J. 2017. Dirigent proteins in plants: modulating cell wall metabolism during abiotic and biotic stress exposure. Journal of Experimental Botany **68**, 3287-3301.

Parmar S, Gharat SA, Tagirasa R, Chandra T, Behera L, Dash SK, Shaw BP. 2020. Identification and expression analysis of miRNAs and elucidation of their role in salt tolerance in rice varieties susceptible and tolerant to salinity. PLOS One. doi: 10.1371/journal.pone.0230958

Pawełkowicz ME, Skarzyńska A, Koter MD, Turek S, Pląder W. 2022. miRNA Profiling and Its Role in Multi-Omics Regulatory Networks Connected with Somaclonal Variation in Cucumber (*Cucumis sativus* L.). International Journal of Molecular Sciences **23**, 4317.

Poorter H, De Jong R. 1999. A comparison of specific leaf area, chemical composition and leaf construction costs of field plants from 15 habitats differing in productivity. New Phytologist **143**, 163-176.

Posit Team. 2024. RStudio: Integrated Development Environment for R. PBC, Boston, MA: Posit Software. http://www.posit.co

Pratyusha DS, Sarada DVL. 2022. MYB transcription factors-master regulators of phenylpropanoid biosynthesis and diverse developmental and stress responses. Plant Cell Reports **41**, 2245-2260.

Pütter J. 1974. Peroxidase. In: Bergmeyer HU (ed) Methods of Enzymatic Analysis. Wenham, MA, USA: Verlag Chemie, 685-690.

Qayyum MA, Bashir F, Maqbool MM, Ali A, Bashir S, Abbas Q. 2019. Implications of Saline Water Irrigation for Linseed on Seed Germination, Seedling Survival and Growth Potential. Sarhad Journal of Agriculture **35**, 1289-1297.

R Core Team. 2024. R: A Language and Environment for Statistical Computing. Vienna, Austria: R Foundation for Statistical Computing. https://www.R-project.org/

Rahneshan Z, Nasibi F, Moghadam AA. 2018. Effects of salinity stress on some growth, physiological, biochemical parameters and nutrients in two pistachio (*Pistacia vera* L.) rootstocks. Journal of Plant Interactions **13**, 73-82.

Ražná K, Harencar L, Kucka M. 2022. The Involvement of microRNAs in Plant Lignan Biosynthesis—Current View. Cells **11**, 2151.

Ražná K, Nozkova J, Vargaova A, Harencar L, Bjelkova M. 2021. Biological Functions of Lignans in Plants. Agriculture (Pol'nohospodárstvo) **67**, 155-165.

Reinhart BJ, Weinstein EG, Rhoades MW, Bartel B, Bartel DP. 2002. MicroRNAs in plants. Genes and Development **16**, 1616-1626.

Reinprecht Y, Perry GE, Peter Pauls K. 2017. A comparison of phenylpropanoid pathway gene families in common bean. Focus on P450 and C4H genes. In: Pérez de la Vega M, Santalla M, Marsolais F, eds. The Common Bean Genome. Cham, Switzerland: Springer International Publishing, 219-261.

Robin AH, Matthew C, Uddin MJ, Bayazid KN. 2016. Salinity-induced reduction in root surface area and changes in major root and shoot traits at the phytomer level in wheat. Journal of Experimental Botany **67**, 3719-3729.

Rodríguez P, Torrecillas A, Morales MA, Ortuño MF, Sánchez-Blanco MJ. 2005. Effects of NaCl salinity and water stress on growth and leaf water relations of *Asteriscus maritimus* plants. Environmental and Experimental Botany **53**, 113-123.

Rodríguez-García C, Sánchez-Quesada C, Toledo E, Delgado-Rodríguez M, Gaforio JJ. 2019. Naturally Lignan-Rich Foods: A Dietary Tool for Health Promotion? Molecules **24**, 917.

Ryser P, Lambers H. 1995. Root and leaf attributes accounting for the performance of fast- and slow-growing grasses at different nutrient supply. Plant and Soil **170**, 251-265.

Sachdev S, Ansari SA, Ansari MI, Fujita M, Hasanuzzaman M. 2021. Abiotic Stress and Reactive Oxygen Species: Generation, Signaling, and Defense Mechanisms. Antioxidants (Basel) **10**, 277.

Saddiq MS, Iqbal S, Hafeez MB, Ibrahim AMH, Raza A, Fatima EM, Baloch H, Jahanzaib, Woodrow P, Ciarmiello LF. 2021. Effect of Salinity Stress on Physiological Changes in Winter and Spring Wheat. Agronomy **11**, 1193.

Sainvitu P, Nott K, Richard G, Blecker C, Jérôme C, Wathelet JP, Paquot M, Deleu M. 2012. Structure, properties and obtention routes of flaxseed lignan secoisolariciresinol: a review. Biotechnology, Agronomy, Society and Environment **16**, 115-124.

Salah IB, Mahmoudi H, Gruber M, Slatni T, Boulaaba T, Gandour M, Messedi D, Hamed KB, Ksouri B, Hannoufa A, Abdelly C. 2011. Phenolic content and antioxidant activity in two contrasting *Medicago ciliaris* lines cultivated under salt stress. Biologia **66**, 813-820.

Šamec D, Karalija E, Šola I, Vujčić Bok V, Salopek-Sondi B. 2021. The Role of Polyphenols in Abiotic Stress Response: The Influence of Molecular Structure. Plants (Basel) **10**, 118.

Sánchés-Moreno C, Larrauri A, Saura-Calixto F. 1998. A procedure to measure the antioxidant efficiency of polyphenols. Journal of the Science of Food and Agriculture **76**, 270-276.

Sarker U, Hossain MN, Oba S, Ercisli S, Marc RA, Golokhvast KS. 2023. Salinity Stress Ameliorates Pigments, Minerals, Polyphenolic Profiles, and Antiradical Capacity in Lalshak. Antioxidants **12**, 173.

Saxena I, Srikanth S, Chen Z. 2016. Cross Talk between H_2O_2 and Interacting Signal Molecules under Plant Stress Response. Frontiers in Plant Science **7**, 570.

Schneider C, Rasband W, Eliceiri K. 2012. NIH Image to ImageJ: 25 years of image analysis. Nature Methods **9**, 671-675.

Sengupta S, Majumder AL. 2009. Insight into the salt tolerance factors of a wild halophytic rice, *Porteresia coarctata*: a physiological and proteomic approach. Planta **229**, 911-929.

Sharma A, Shahzad B, Rehman A, Bhardwaj R, Landi M, Zheng B. 2019. Response of Phenylpropanoid Pathway and the Role of Polyphenols in Plants under Abiotic Stress. Molecules **24**, 2452.

Shafrin F, Das SS, Sanan-Mishra N, Khan H. 2015. Artificial miRNA-mediated down-regulation of two monolignoid biosynthetic genes (C3H and F5H) cause reduction in lignin content in jute. Plant Molecular Biology **89**, 511-527.

Shuai P, Su Y, Liang D, Zhang Z, Xia X, Yin W. 2016. Identification of phasiRNAs and their drought- responsiveness in *Populus trichocarpa*. FEBS Letter **590**, 3616-3627.

Siddiqui ZS, Asim N, Uddin Z. 2022. Interactive Effect of Organic (Urea-N) and Halo (NaCl) Priming on Photosystem II Efficiencies and Physiological Tolerance in Flax Plants under Saline Environment. Russian Journal of Plant Physiology **69**, 102.

Singh DK, Mehra S, Chatterjee S, Purty RS. 2020. In silico identification and validation of miRNA and their DIR specific targets in *Oryza sativa* Indica under abiotic stress. Non-coding RNA Research **5**, 167-177.

Singh N, Srivastava S, Sharma A. 2016. Identification and analysis of miRNAs and their targets in ginger using bioinformatics approach. Gene **575**, 570-576.

Singh PK, Singh R, Singh S. 2013. Cinnamic acid induced changes in reactive oxygen species scavenging enzymes and protein profile in maize (*Zea mays* L.) plants grown under salt stress. Physiology and Molecular Biology of Plants **19**, 53-59.

Sinha AK. 1972. Colorimetric assay of catalase. Analytical Biochemistry **47**, 389-394.

Singleton VL, Rossi JA. 1965. Colorimetry of total phenolics with phosphomolybdic-phosphotungstic acid reagents. American Journal of Enology and Viticulture **16**, 144-158.

Slama I, M'Rabet R, Ksouri R, Talbi O, Debez A, Abdelly C. 2017. Effects of salt treatment on growth, lipid membrane peroxidation, polyphenol content, and antioxidant activities in leaves of *Sesuvium portulacastrum* L. Arid Land Research and Management **31**, 404-417.

Smirnoff N, Cumbes QJ. 1989. Hydroxyl radical scavenging activity of compatible solutes. Phytochemistry **28**, 1057-1060.

Stehlo P, Ková K. 2023. Country report on the present environmental situation in agriculture – Slovakia. https://www.fao.org/3/x3413e/x3413e19.htm Accessed October 2024

Sun P, Cheng C, Lin Y, Zhu Q, Lin J, Lai Z. 2017. Combined small RNA and degradome sequencing reveals complex microRNA regulation of catechin biosynthesis in tea (*Camellia sinensis*). PLOS One **12**, e0171173.

Sunkar R, Li Y-F, Jagadeeswaran G. 2012. Functions of micro-RNAs in plant stress responses. Trends in Plant Science **17**, 196-203.

Tang H, Niu L, Wei J, Chen X, Chen Y. 2019. Phosphorus Limitation Improved Salt Tolerance in Maize Through Tissue Mass Density Increase, Osmolytes Accumulation, and Na+ Uptake Inhibition. Frontiers in Plant Science **10**, 856.

Tao R, Ding J, Li C, Zhu X, Guo W, Zhu M. 2021. Evaluating and Screening of Agro-Physiological Indices for Salinity Stress Tolerance in Wheat at the Seedling Stage. Frontiers in Plant Science **12**, 646175.

Telesiński A, Nowak J, Smolik B, Dubowska A, Skrzypiec N. 2008. Effect of soil salinity on activity of antioxidant enzymes and content of ascorbic acid and phenols in bean (*Pheseolus vulgaris* L.) plants. Journal of Elementology **13**, 401-409.

Teponno RB, Kusari S, Spiteller M. 2016. Recent advances in research on lignans and neolignans. Natural Product Reports **33**, 1044-1092.

Tractor Junction. 2022. Soil Salinity In India: The Reasons, Effects, and Solutions. https://www.tractorjunction.com/blog/soil-salinity-in-india-the-reasons-effects-and-solutions/ Accessed October 2024

Truong DH, Lan Nguyen TH, Dao DQ. 2023. Revisiting the $HO^{\bullet}$-initiated oxidation of L-proline amino acid in the aqueous phase: influence of transition metal ions. Royal Society Open Science **10**, 230114.

Tu Z, Xia H, Yang L, Zhai X, Shen Y, Li H. 2022. The Roles of microRNA-Long Non-coding RNA-mRNA Networks in the Regulation of Leaf and Flower Development in *Liriodendron chinense*. Frontiers in Plant Science **13**, 816875.

Türkan I, Demiral T. 2009. Recent developments in understanding salinity tolerance. Environmental and Experimental Botany **67**, 2-9.

Turner NC. 1986. Crop Water Deficits: A Decade of Progress. In: Brady NC, ed. Advances in Agronomy, Volume 39. USA: Elsevier, 1-51.

Ueda A, Kanechi M, Uno Y, Inagaki N. 2003. Photosynthetic limitations of a halophyte sea aster (*Aster tripolium* L) under water stress and NaCl stress. Journal of Plant Research **116**, 65-70.

UN. 2024. United Nations. The 17 Goals. https://sdgs.un.org/goals/ Accessed October 2024

Varga I, Tkalec Kojić M, Iljkić D, Rastija M, Antunović M. 2020. Fiber flax germination at different temperatures and salinity stress conditions. Sjemenarstvo. 31. doi: 10.33128/s1.31.1-2.2

Vasilakoglou I, Dhima K, Giannakoula A, Dordas C, Skiada V, Papadopoulou K. 2021. Carbon Assimilation, Isotope Discrimination, Proline and Lipid Peroxidation Contribution to Barley (*Hordeum vulgare*) Salinity Tolerance. Plants **10**, 299.

Vijayalakshmi T, Vijayakumar AS, Kiranmai K, Nareshkumar A, Sudhakar C. 2016. Salt Stress Induced Modulations in Growth, Compatible Solutes and Antioxidant Enzymes Response in Two Cultivars of Safflower (*Carthamus tinctorius* L. Cultivar TSF1 and Cultivar SM) Differing in Salt Tolerance. American Journal of Plant Sciences **7**, 1802-1819.

Wang M, Wang Y, Zhang Y, Li C, Gong S, Yan S, Li G, Hu G, Ren H, Yang J, Yu T, Yang K. 2019. Comparative transcriptome analysis of salt-sensitive and salt-tolerant maize reveals potential mechanisms to enhance salt resistance. Genes and Genomics **41**, 781-801.

Wang H, Liang L, Liu S, An T, Fang Y, Xu B, Zhang S, Deng X, Palta JA, Siddique KHM, Chen Y. 2020. Maize genotypes with deep root systems tolerate salt stress better than those with shallow root systems during early growth. Journal of Agronomy and Crop Science **206**, 711-721.

Wang H, Wang X, Li Y, Cui Y, Yan X, Gao J, Ouyang J, Li S. 2024. Pleiotropic Effects of miR5504 Underlying Plant Height, Grain Yield and Quality in Rice. Plant and Cell Physiology **65**, 781-789.

Wang N, Lin Y, Qi F, Xiaoyang C, Peng Z, Yu Y, Liu Y, Zhang J, Qi X, Deyholos M, Zhang J. 2022. Comprehensive Analysis of Differentially Expressed Genes and Epigenetic Modification-Related Expression Variation Induced by Saline Stress at Seedling Stage in Fiber and Oil Flax, *Linum usitatissimum* L. Plants (Basel) **11**, 2053.

Wei K, Chen H. 2018. Global identification, structural analysis and expression characterization of cytochrome P450 monooxygenase superfamily in rice. BMC Genomics **19**, 35.

West G, Inzé D, Beemster GT. 2004. Cell cycle modulation in the response of the primary root of Arabidopsis to salt stress. Plant Physiology **135**, 1050-1058.

Yadav B, Kaur V, Narayan OP, Yadav SK, Kumar A, Wankhede DP. 2022. Integrated omics approaches for flax improvement under abiotic and biotic stress: Current status and future prospects. Frontiers in Plant Science **13**, 931275.

Xia K, Pan X, Chen H, Xu X, Zhang M. 2023. Rice miR168a-5p regulates seed length, nitrogen allocation and salt tolerance by targeting *OsOFP3*, *OsNPF2.4* and *OsAGO1a*, respectively. Journal of Plant Physiology **280**, 153905.

Xie D, Yang X, He R, Ren X, Huo H, Yuan H, Wu G, Su J, Sun J. 2023. Identification of regulatory pathways of miRna and phasiRna related to flax lignan synthesis. Journal of Natural Fibers **20**, 2185426.

Yadav N, Sawariya M, Kumar A, Mehra H, Sharma J, Kumar S, Devi S, Kaur V, Arya SS. 2024. Influence of GA3 (gibberellic acid) and Ca(calcium) on root trait variation and osmotic potential of linseed (*Linum usitatissimum* L.) under chloride-dominated salinity. Journal of Applied and Natural Science **16**, 271-281.

Yan F, Li H, Zhao P. 2019. Genome-Wide Identification and Transcriptional Expression of the *PAL* Gene Family in Common Walnut (*Juglans Regia* L.). Genes **10**, 46.

Yan S, Weng B, Jing L, Bi W. 2023. Effects of drought stress on water content and biomass distribution in summer maize (*Zea mays* L.). Frontiers in Plant Science **14**, 1118131.

Yang Y, Guo Y. 2018. Unraveling salt stress signaling in plants. Journal of Integrative Plant Biology **60**, 796-804.

Yaşar M. 2023. Sensitivity of different flax (*Linum usitatissimum* L.) genotypes to salinity determined by GE biplot. Saudi Journal of Biological Sciences **30**, 103592.

Yildiz M, Poyraz İ, Çavdar A, Özgen Y, Beyaz R. 2020. Plant Responses to Salt Stress. In: Abdurakhmonov IY, ed. Plant Breeding - Current and Future Views. London, UK: IntechOpen.

Yildrim E, Donmez M F, Turan M. 2008. Use of Bioinoculants in Ameliorative Effects on Radish Plants Under Salinity Stress. Journal of Plant Nutrition **31**, 2059-2074.

Yuan Q, Zhang J, Wang S, Zhang M, Nie J. 2024. Identification, evolution and expression analysis of the UDP-glycosyltransferase gene family in cucumber (*Cucumis sativus* L.). Scientia Horticulturae **324**, 112615.

Zeeshan M, Lu M, Sehar S, Holford P, Wu F. 2020. Comparison of Biochemical, Anatomical, Morphological, and Physiological Responses to Salinity Stress in Wheat and Barley Genotypes Deferring in Salinity Tolerance. Agronomy **10**, 127.

Zeki Koçak M, Göre M, Kurt O. 2022. The Effect of Different Salinity Levels on Germination Development of Some Flax (*Linum usitatissimum* L.) Varieties. Turkish Journal of Agriculture - Food Science and Technology **10**, 657-662.

Zhang B. 2015. MicroRNA: a new target for improving plant tolerance to abiotic stress. Journal of Experimental Botany **66**, 1749-1761.

Zhang B, Wang Q, Wang K, Pan X, Liu F, Guo T, Cobb GP, Anderson TA. 2007. Identification of cotton microRNAs and their targets. Gene **397**, 26-37.

Zhang C, Xu X, Xu X, Li Y, Zhao P, Chen X, Shen X, Zhang Z, Chen Y, Liu S, XuHan X, Lin Y, Lai Z. 2022. Genome-wide identification, evolution analysis of *cytochrome*

P450 monooxygenase multigene family and their expression patterns during the early somatic embryogenesis in *Dimocarpus longan* Lour. Gene **826**, 146453.

Zhao S, Zhang Q, Liu M, Zhou H, Ma C, Wang P. 2021. Regulation of Plant Responses to Salt Stress. International Journal of Molecular Sciences **22**, 4609.

Zoclanclounon YAB, Rostás M, Chung NJ, Mo Y, Karlovsky P, Dossa K. 2022. Characterization of Peroxidase and Laccase Gene Families and In Silico Identification of Potential Genes Involved in Upstream Steps of Lignan Formation in Sesame. Life (Basel) **12**, 1200.

TABLE

Table 1 Ratio of different shoot and root parameters of two flax genotypes Flanders and Astella under 100 mM NaCl treatment. The data were estimated as relative changes under the stress period, normalised against control treatment. The ratios of normalised relative values are represented in this table. The ratios of control treatment values are omitted. *RL* root length, *SL* shoot length, *RFW* root fresh weight, *SFW* shoot fresh weight, *RDW* root dry weight, *SDW* shoot dry weight, *RRWC* root relative water content, *SRWC* shoot relative water content.

Genotype	**RL/SL**	**RFW/SFW**	**RDW/SDW**	**RRWC/SRWC**
Flanders	1.01	1.35	1.16	1.01
Astella	2.12	1.35	1.02	1.03

FIGURE LEGENDS AND ALTERNATIVE TEXTS FOR ACCESSIBILITY

Fig. 1. Relative changes of several morphological parameters of two flax varieties, Flanders and Astella, under one week of 100 mM NaCl stress. Data represent relative changes during the stress period, except for leaf relative water content, measured at the end of NaCl stress. Data were normalised to the control treatment. (A-C) Relative changes in Shoot length, root length and diameter (A), root volume (B), and root tips and forks (C) in Flanders and Astella. A photographic representation of comparative morphology between Flanders and Astella in control and stressed conditions (scale bar = 10 mm) (D.1-D.2). (E-I) Relative changes in leaf number (E), relative water contents of shoot and root (F), leaf relative water content (G), fresh and dry weights of shoots and roots (H), and root density (I) in Flanders and Astella. Data represent mean ± standard errors (n = 3) of three biological and three technical replicates. Different letters represent statistical differences at $p < 0.05$ (one-way ANOVA with DMRT post hoc test).

Fig. 1 alternative text. Eight double bar graphs show the relative changes in shoot length, root length, root diameter, root volume, root tip numbers, root fork numbers, leaf numbers, shoot water content, root water content, leaf water content, shoot fresh weight, root fresh weight, shoot dry weight, root dry weight, and root mass density under zero and hundred millimolar one-week sodium chloride salt-stressed flax varieties Flanders and Astella.

Fig. 1A. Relative changes in shoot length.

Genotype	Salt concentration	Shoot length	Standard error
Flanders	0 millimolar sodium chloride	10 centimetres	0.89726
Flanders	100 millimolar sodium chloride	7.92079 centimetres	0.71611
Astella	0 millimolar sodium chloride	10 centimetres	0.89125
Astella	100 millimolar sodium chloride	8.11321 centimetres	0.53575

Fig. 1A. Relative changes in root length.

Genotype	Salt concentration	Root length	Standard error
Flanders	0 millimolar sodium chloride	10 centimetres	0.96252
Flanders	100 millimolar sodium chloride	7.98786 centimetres	0.71698
Astella	0 millimolar sodium chloride	10 centimetres	0.9035
Astella	100 millimolar sodium chloride	17.18126 centimetres	1.12587

Fig. 1A. Relative changes in root diameter.

Genotype	Salt concentration	Root diameter	Standard error
Flanders	0 millimolar sodium chloride	-10 centimetres	0.48904
Flanders	100 millimolar sodium chloride	-10.67571 centimetres	0.55258
Astella	0 millimolar sodium chloride	-10 centimetres	0.34647
Astella	100 millimolar sodium chloride	-25.69408 centimetres	1.09694

Fig. 1B. Relative changes in root volume.

Genotype	Salt concentration	Root volume	Standard error
Flanders	0 millimolar sodium chloride	10 cubic millimetres	0.60131
Flanders	100 millimolar sodium chloride	1.89394 cubic millimetres	0.58682
Astella	0 millimolar sodium chloride	10 cubic millimetres	1.24482
Astella	100 millimolar sodium chloride	7.04545 cubic millimetres	0.98412

Fig. 1C. Relative changes in root tip numbers.

Genotype	Salt concentration	Root tips	Standard error
Flanders	0 millimolar sodium chloride	10	0.96925
Flanders	100 millimolar sodium chloride	2.67045	0.49206
Astella	0 millimolar sodium chloride	10	0.83034
Astella	100 millimolar sodium chloride	14.27966	0.77323

Fig. 1C. Relative changes in root fork numbers.

Genotype	Salt concentration	Root forks	Standard error
Flanders	0 millimolar sodium chloride	10	0.87051
Flanders	100 millimolar sodium chloride	7.29412	0.50943
Astella	0 millimolar sodium chloride	10	0.77728
Astella	100 millimolar sodium chloride	9.25	0.54006

Fig. 1D.1. shows the stunted overall growth of salt stresses Flanders.

Fig. 1D.2. depicts a similar shoot length of salt-stressed Astella to that of non-stressed Astella, but the root of the stressed Astella is longer than that of non-stressed Astella.

Fig. 1E. Relative changes in leaf numbers.

Genotype	Salt concentration	Leaf number	Standard error
Flanders	0 millimolar sodium chloride	10	0.79111
Flanders	100 millimolar sodium chloride	9.80952	1.49375
Astella	0 millimolar sodium chloride	10	0.8231
Astella	100 millimolar sodium chloride	5.46875	1.46367

Fig. 1F. Relative changes in shoot water content.

Genotype	Salt concentration	Shoot water content	Standard error
Flanders	0 millimolar sodium chloride	10 percentage	0.09865
Flanders	100 millimolar sodium chloride	10.29274 percentage	0.04665
Astella	0 millimolar sodium chloride	10 percentage	0.0908
Astella	100 millimolar sodium chloride	9.93549 percentage	0.22567

Fig. 1F. Relative changes in root water content.

Genotype	Salt concentration	Root water content	Standard error
Flanders	0 millimolar sodium chloride	10 percentage	0.11069
Flanders	100 millimolar sodium chloride	10.34698 percentage	0.0486
Astella	0 millimolar sodium chloride	10 percentage	0.18734
Astella	100 millimolar sodium chloride	10.23805 percentage	0.10553

Fig. 1G. Relative changes in leaf relative water content.

Genotype	Salt concentration	Leaf relative water content	Standard error
Flanders	0 millimolar sodium chloride	10 percentage	0.37615
Flanders	100 millimolar sodium chloride	10.52312 percentage	0.24552
Astella	0 millimolar sodium chloride	10 percentage	0.47908
Astella	100 millimolar sodium chloride	9.29317 percentage	0.26697

Fig. 1H. Relative changes in shoot fresh weight.

Genotype	Salt concentration	Shoot fresh weight	Standard error
Flanders	0 millimolar sodium chloride	10 milligrams	0.4518
Flanders	100 millimolar sodium chloride	6.10627 milligrams	0.33898
Astella	0 millimolar sodium chloride	10 milligrams	0.23587
Astella	100 millimolar sodium chloride	4.27003 milligrams	0.24241

Fig. 1H. Relative changes in root fresh weight.

Genotype	Salt concentration	Root fresh weight	Standard error
Flanders	0 millimolar sodium chloride	10 milligrams	0.41733
Flanders	100 millimolar sodium chloride	8.23266 milligrams	0.48085
Astella	0 millimolar sodium chloride	10 milligrams	0.74039
Astella	100 millimolar sodium chloride	5.75209 milligrams	0.95493

Fig. 1H. Relative changes in shoot dry weight.

Genotype	Salt concentration	Shoot dry weight	Standard error
Flanders	0 millimolar sodium chloride	10 milligrams	0.50631
Flanders	100 millimolar sodium chloride	4.63918 milligrams	0.34808
Astella	0 millimolar sodium chloride	10 milligrams	0.54804
Astella	100 millimolar sodium chloride	4.52465 milligrams	0.71449

Fig. 1H. Relative changes in root dry weight.

Genotype	Salt concentration	Root dry weight	Standard error
Flanders	0 millimolar sodium chloride	10 milligrams	1.1177
Flanders	100 millimolar sodium chloride	5.36585 milligrams	0.59744
Astella	0 millimolar sodium chloride	10 milligrams	1.79029
Astella	100 millimolar sodium chloride	4.61538 milligrams	0.86003

Fig. 1I. Relative changes in root mass density

Genotype	Salt concentration	Root mass density	Standard error
Flanders	0 millimolar sodium chloride	10 milligrams per cubic millimetre	0.44904
Flanders	100 millimolar sodium chloride	59.34525 milligrams per cubic millimetre	21.17334
Astella	0 millimolar sodium chloride	10 milligrams per cubic millimetre	1.56677
Astella	100 millimolar sodium chloride	8.29881 milligrams per cubic millimetre	2.08573

Fig. 2. The estimation of reactive oxygen species (ROS) and associated cell damages in two flax varieties Flanders and Astella after one week of 100 mM NaCl stress. In our study, we represented hydrogen peroxide (H_2O_2) as the ROS marker (A) and, Malondialdehyde (MDA) content as the cell damage marker (B). ROS is a regular byproduct of cellular metabolism. Antioxidants scavenge ROS molecules to create a neutral redox potential inside the cell. ROS overproduction during salt stress disturbs the redox state of the affected cells, generating the "oxidative burst" situation. Excessive ROS molecules damage lipid bilayer membranes by lipid oxidation generating MDA as the end-product. Data represent mean ± standard errors (n = 3) of three biological and three technical replicates. Different letters represent statistical differences at $p < 0.05$ (one-way ANOVA with DMRT post hoc test).

Fig. 2 alternative text. Two double bar graphs show the hydrogen peroxide, and malondialdehyde amounts generated under zero and hundred millimolar one-week sodium chloride salt-stressed flax varieties Flanders and Astella.

Fig. 2A.

Genotype	Salt concentration	Hydrogen peroxide	Standard error
Flanders	0 millimolar sodium chloride	5.53511 micromole per gram of fresh weight	0.12562
Flanders	100 millimolar sodium chloride	19.71467 micromole per gram of fresh weight	0.79514
Astella	0 millimolar sodium chloride	5.20189 micromole per gram of fresh weight	0.09253
Astella	100 millimolar sodium chloride	39.62333 micromole per gram of fresh weight	0.73779

Fig. 2B.

Genotype	Salt concentration	Malondialdehyde	Standard error
Flanders	0 millimolar sodium chloride	2.02611 micromole per gram of fresh weight	0.05947
Flanders	100 millimolar sodium chloride	7.51144 micromole per gram of fresh weight	0.16012
Astella	0 millimolar sodium chloride	2.56278 micromole per gram of fresh weight	0.2065
Astella	100 millimolar sodium chloride	14.27556 micromole per gram of fresh weight	0.58882

Fig. 3. The estimation of enzymatic antioxidants in two flax varieties Flanders and Astella after one week of 100 mM NaCl stress. In response to the salt stress-mediated "oxidative burst", plants activate a well-synchronised antioxidant system for ROS scavenging. (A) The frontline defence is provided by superoxide dismutase (SOD) by converting superoxide ($O_2^{\bullet-}$) to H_2O_2; catalase (CAT) (B), ascorbate peroxidase (APX) (C), and guaiacol peroxidase (GPOX) (D) converts H_2O_2 to H_2O and O_2. Data represent mean ± standard errors (n = 3) of three biological and three technical replicates. Different letters represent statistical differences at $p < 0.05$ (one-way ANOVA with DMRT post hoc test).

Fig. 3 alternative text. Four double bar graphs show the superoxide dismutase, catalase, ascorbate peroxidase, and guaiacol peroxidase amounts generated under zero and hundred millimolar one-week sodium chloride salt-stressed flax varieties Flanders and Astella.

Fig. 3A.

Genotype	Salt concentration	Superoxide dismutase	Standard error
Flanders	0 millimolar sodium chloride	0.09111 units per milligram of protein	0.00196
Flanders	100 millimolar sodium chloride	0.25356 units per milligram of protein	0.00592
Astella	0 millimolar sodium chloride	0.084 units per milligram of protein	0.00504
Astella	100 millimolar sodium chloride	0.18633 units per milligram of protein	0.00362

Fig. 3B.

Genotype	Salt concentration	Catalase	Standard error
Flanders	0 millimolar sodium chloride	0.11522 units per gram of protein	0.00388
Flanders	100 millimolar sodium chloride	1.47344 units per gram of protein	0.04618
Astella	0 millimolar sodium chloride	0.12944 units per gram of protein	0.00329
Astella	100 millimolar sodium chloride	0.91811 units per gram of protein	0.02736

Fig. 3C.

Genotype	Salt concentration	Ascorbate peroxidase	Standard error
Flanders	0 millimolar sodium chloride	0.00901 units per gram of protein	0.000410059
Flanders	100 millimolar sodium chloride	0.02551 units per gram of protein	0.00127
Astella	0 millimolar sodium chloride	0.00763 units per gram of protein	0.000439275
Astella	100 millimolar	0.0183 units per gram of protein	0.000639155

	sodium chloride		

Fig. 3D.

Genotype	Salt concentration	Guaiacol peroxidase	Standard error
Flanders	0 millimolar sodium chloride	0.21911 units per gram of protein	0.00485
Flanders	100 millimolar sodium chloride	0.99156 units per gram of protein	0.01855
Astella	0 millimolar sodium chloride	0.19833 units per gram of protein	0.00278
Astella	100 millimolar sodium chloride	0.643 units per gram of protein	0.00219

Fig. 4. The estimation of non-enzymatic antioxidants, total radical scavenging activity, and proline content in two flax varieties Flanders and Astella after one week of 100 mM NaCl stress. The non-enzymatic antioxidants polyphenols (A) and phenolic acids (B) are excellent antioxidants due to the presence of multiple hydroxyl groups. (C) The total radical scavenging activity was measured using DPPH assay. (D) Proline provides cellular protection against salt stress in multiple ways. Data represent mean ± standard errors (n = 3) of three biological and three technical replicates. Different letters represent statistical differences at $p < 0.05$ (one-way ANOVA with DMRT post hoc test).

Fig. 4 alternative text. Four double bar graphs show the polyphenols, phenolic acids, D P P H, and proline amounts generated under zero and hundred millimolar one-week sodium chloride salt-stressed flax varieties Flanders and Astella.

Fig. 4A.

Genotype	Salt concentration	Polyphenols	Standard error
Flanders	0 millimolar sodium chloride	4.09548 milligrams per litre of gallic acid	0.36159
Flanders	100 millimolar sodium chloride	5.55775 milligrams per litre of gallic acid	0.28544
Astella	0 millimolar sodium chloride	3.72444 milligrams per litre of gallic acid	0.30511
Astella	100 millimolar sodium chloride	2.34249 milligrams per litre of gallic acid	0.37002

Fig. 4B.

Genotype	Salt concentration	Phenolic acids	Standard error
Flanders	0 millimolar sodium chloride	4.55112 milligrams per gram of caffeic acid	0.3829
Flanders	100 millimolar sodium chloride	4.97933 milligrams per gram of caffeic acid	0.55545
Astella	0 millimolar sodium chloride	2.59168 milligrams per gram of caffeic acid	0.43613
Astella	100 millimolar sodium chloride	1.33157 milligrams per gram of caffeic acid	0.44157

Fig. 4C.

Genotype	Salt concentration	D P P H	Standard error
Flanders	0 millimolar sodium chloride	1.82186 milligrams per gram of Trolox	0.10473
Flanders	100 millimolar sodium chloride	2.41146 milligrams per gram of Trolox	0.16735
Astella	0 millimolar sodium chloride	1.92083 milligrams per gram of Trolox	0.20912
Astella	100 millimolar	1.11597 milligrams per gram of	0.22755

	sodium chloride	Trolox	

Fig. 4D.

Genotype	Salt concentration	Proline	Standard error
Flanders	0 millimolar sodium chloride	0.77689 micromole per gram of fresh weight	0.04616
Flanders	100 millimolar sodium chloride	9.91011 micromole per gram of fresh weight	0.16062
Astella	0 millimolar sodium chloride	0.68811 micromole per gram of fresh weight	0.03524
Astella	100 millimolar sodium chloride	6.58911 micromole per gram of fresh weight	0.15136

Fig. 5. The expression of lignan-miRNAs in two flax varieties Flanders and Astella after one week of 100 mM NaCl stress. The mRNAs were isolated from treatment plants and the relative expressions of miR168a (A), miR399g (B), and miR828a (C) were measured using the two-tailed qPCR assay kit using Cyklophilin and ETIF5A as internal controls for normalisation. Data represent mean ± standard errors (n = 3) of three biological and three technical replicates. Different letters represent statistical differences at $p < 0.05$ (one-way ANOVA with DMRT post hoc test).

Fig. 5 alternative text. Three double bar graphs show the expressions of microRNA 168 a, microRNA 399 g, and microRNA 828 a under zero and hundred millimolar one-week sodium chloride salt-stressed flax varieties Flanders and Astella.

Fig. 5A. MicroRNA 168 a.

Genotype	Salt concentration	Fold change	Standard error
Flanders	0 millimolar sodium chloride	1	0.62375
Flanders	100 millimolar sodium chloride	8.30767	0.57784
Astella	0 millimolar sodium chloride	1	0.53872
Astella	100 millimolar sodium chloride	3.24026	0.62273

Fig. 5B. MicroRNA 399 g.

Genotype	Salt concentration	Fold change	Standard error
Flanders	0 millimolar sodium chloride	1	0.41502
Flanders	100 millimolar sodium chloride	13.00605	0.31829
Astella	0 millimolar sodium chloride	1	0.2851
Astella	100 millimolar sodium chloride	6.53063	0.28738

Fig. 5C. MicroRNA 828 a.

Genotype	Salt concentration	Fold change	Standard error
Flanders	0 millimolar sodium chloride	1	0.37766
Flanders	100 millimolar sodium chloride	5.84283	0.38716
Astella	0 millimolar sodium chloride	1	0.48417
Astella	100 millimolar sodium chloride	3.11066	0.39043

Fig. 6. Fluorescence microscopic study of root cell viability of flax varieties Flanders and Astella using FDA-PI differential staining after one week of 100 mM NaCl stress. Alive cells were green and dead cells were red. (A), (C), (E), and (G) are Flanders roots. (B), (D), (F), and (H) are Astella roots. Root tips (blue arrows in figures (A) and (B)) and lateral root buds (blue arrows in figures (C) and (D)) were alive in both genotypes. The root epidermal layer was mostly dead (yellow arrows in figures (A), (B), (C), and (D)). A sporadic pattern of live cells was found in the root maturation zone (white arrows in figures (E) and (F)). Cross-sectional views also depicted the dead epidermal layer (E in figures (G) and (H)). *E* epidermis, *C* cortex, *E/P* endodermis/pericycle, *X* xylem, *F* phloem.

Fig. 6 alternative text. FDA-PI differential-stained one-week sodium chloride salt-stressed roots of Flanders and Astella depict signs of salinity stress-mediated root damages.

Fig. 7. Correlation analyses using Pearson's correlation (PCC) analysis and principal component analysis (PCA) of the experimental results obtained after providing 100 mM NaCl stress for one week on two flax varieties Flanders and Astella. (A) PCC analysis. We represented the correlation constants as pie figures and the percentage of the correlation values as numbers in the plot. (B) PCA plot represents the loading values of different variables measured in this study. PC1 and PC2 described a total of 84.79% variation.

Fig. 7 alternative text. Two diagrams show Pearson's correlation coefficient and principal component analysis of the independent variables used in the study.

Fig. 7A. Pearson's correlation coefficient analysis revealed correlation of H_2O_2 with proline (100 per cent), Catalase (95 per cent), ascorbate peroxidase (80 per cent), phenolic acids (73 per cent), microRNA 168 a (83 per cent), microRNA 399 g (91 per cent), microRNA 828 a (90 per cent), and Malondialdehyde (54%), and negatively correlated with majority morphological markers. Malondialdehyde was moderately correlated with proline (54 per cent), and negatively correlated with the morphological markers.

Fig. 7B. Principal component analysis revealed a total principal component 1 and principal component 2 variance of 84.79 per cent.

Fig. 8. A speculative representation of flax salt stress mitigation strategy, based on the evidences found in this study. In flax, salt stress-induced ROS can upregulate antioxidants (AA) except polyphenols (PP) and the expression of lignan-related miRNAs (miR). A homeostasis may exist between AA, miR, and PP where AA and miR can upregulate each other, and both can downregulate PP. The grey oval shape highlights the homeostatic relationship. AA and miR can downregulate both ROS and cell damage. ROS promotes cell damage. However, ROS-mediated cell damage remains moderate due to the joint inhibition effect of AA and miR. Plant growth is inhibited by four factors: ROS, AA, miR, and cell damage. AA and PP are connected with growth via the numbers 1 and 2, respectively, written in the red circles. Upregulations and downregulations are represented by solid green and red lines, respectively. The dashed green line represents moderate upregulation. Question marks (?) represent speculative regions.

Fig. 8 alternative text. A diagram shows salt stress-mediated reactive oxygen species generation and its relation with antioxidants, microRNAs, polyphenols, cell damage, and plant growth in flax varieties Flanders and Astella. We speculate a hypothetical homeostasis between antioxidants, microRNAs, and polyphenols that aids salt stress mitigation strategy in flax.

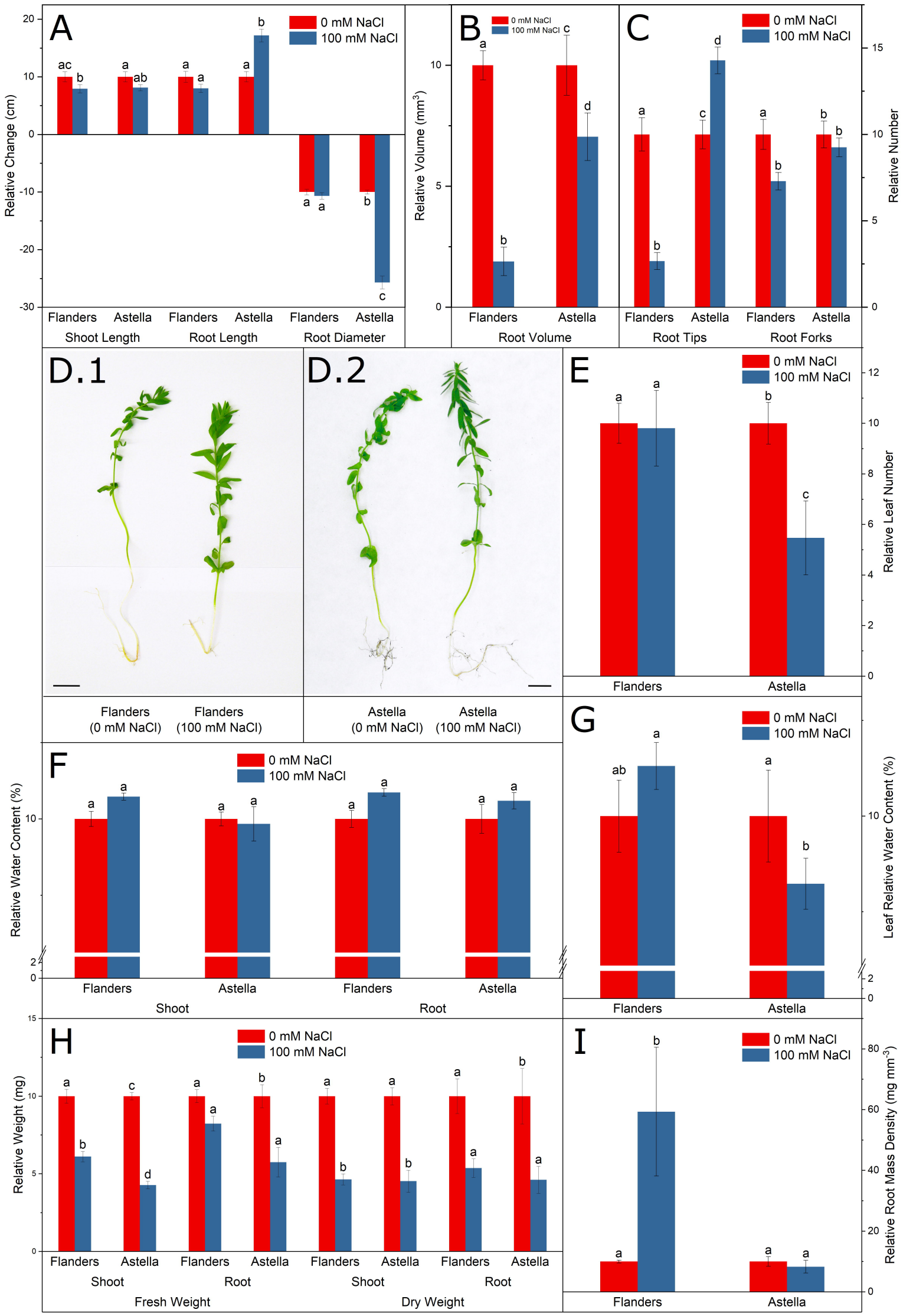

Fig. 1. Relative changes of several morphological parameters of two flax varieties, Flanders and Astella, under one week of 100 mM NaCl stress. Data represent relative changes during the stress period, except for leaf relative water content, measured at the end of NaCl stress. Data were normalised to the control treatment. (A-C) Relative changes in Shoot length, root length and diameter (A), root volume (B), and root tips and forks (C) in Flanders and Astella. A photographic representation of comparative morphology between Flanders and Astella in control and stressed conditions (scale bar = 10 mm) (D.1-D.2). (E-I) Relative changes in leaf number (E), relative water contents of shoot and root (F), leaf relative water content (G), fresh and dry weights of shoots and roots (H), and root density (I) in Flanders and Astella. Data represent mean ± standard errors (n = 3) of three biological and three technical replicates. Different letters represent statistical differences at $p < 0.05$ (one-way ANOVA with DMRT post hoc test).

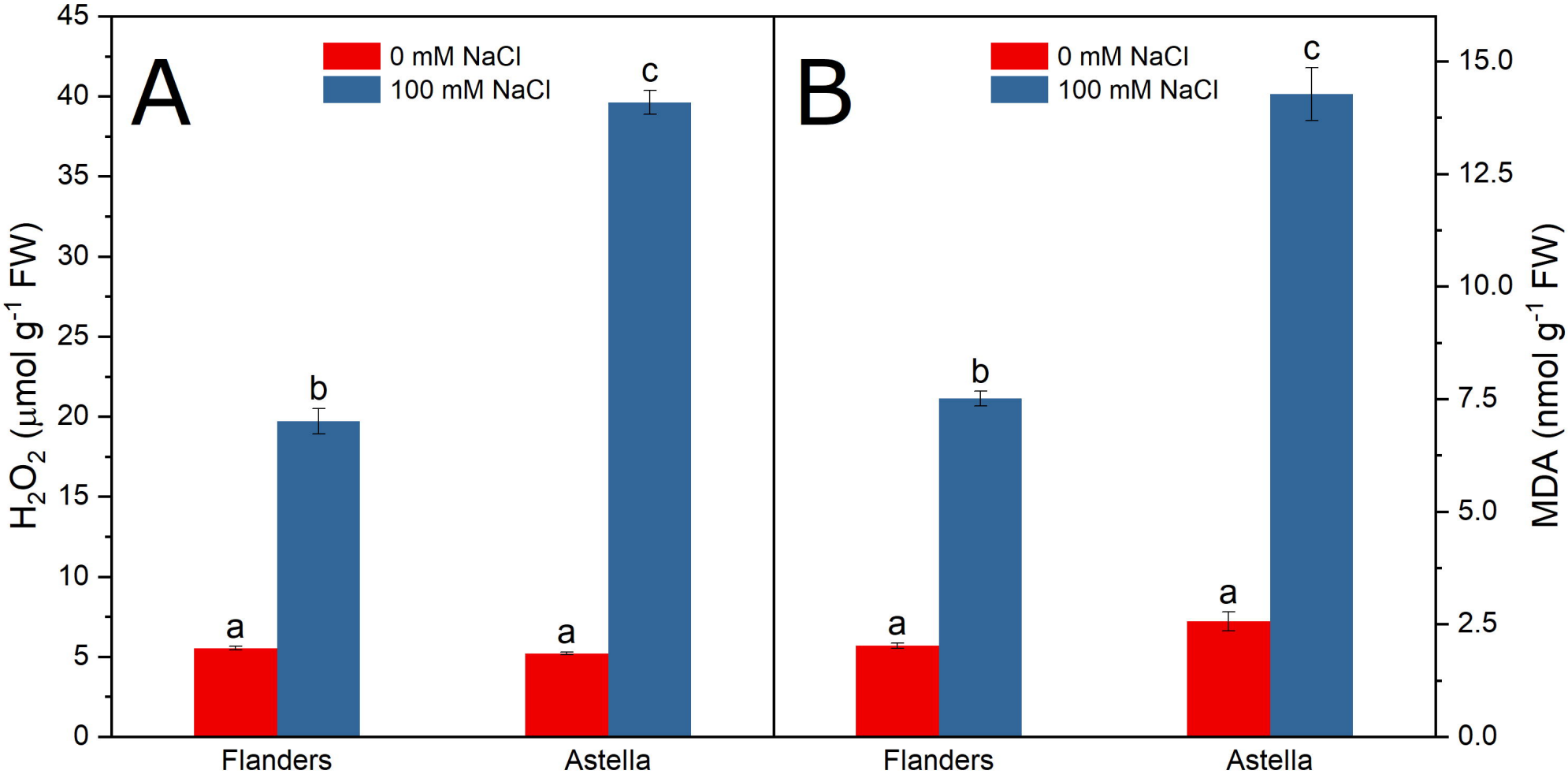

Fig. 2. The estimation of reactive oxygen species (ROS) and associated cell damages in two flax varieties Flanders and Astella after one week of 100 mM NaCl stress. In our study, we represented hydrogen peroxide (H2O2) as the ROS marker (A) and, Malondialdehyde (MDA) content as the cell damage marker (B). ROS is a regular byproduct of cellular metabolism. Antioxidants scavenge ROS molecules to create a neutral redox potential inside the cell. ROS overproduction during salt stress disturbs the redox state of the affected cells, generating the "oxidative burst" situation. Excessive ROS molecules damage lipid bilayer membranes by lipid oxidation generating MDA as the end-product. Data represent mean ± standard errors (n = 3) of three biological and three technical replicates. Different letters represent statistical differences at $p < 0.05$ (one-way ANOVA with DMRT post hoc test).

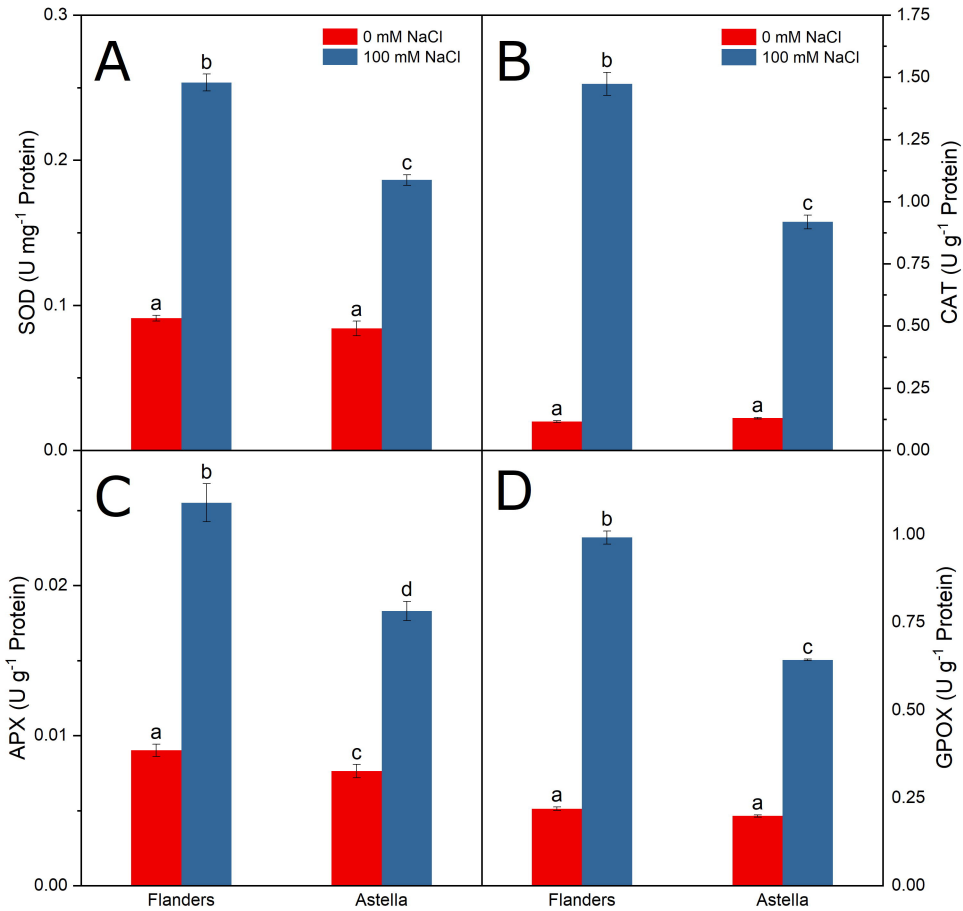

Fig. 3. The estimation of enzymatic antioxidants in two flax varieties Flanders and Astella after one week of 100 mM NaCl stress. In response to the salt stress-mediated "oxidative burst", plants activate a well-synchronised antioxidant system for ROS scavenging. (A) The frontline defence is provided by superoxide dismutase (SOD) by converting superoxide (O2•−) to H2O2; catalase (CAT) (B), ascorbate peroxidase (APX) (C), and guaiacol peroxidase (GPOX) (D) converts H2O2 to H2O and O2. Data represent mean ± standard errors (n = 3) of three biological and three technical replicates. Different letters represent statistical differences at $p < 0.05$ (one-way ANOVA with DMRT post hoc test).

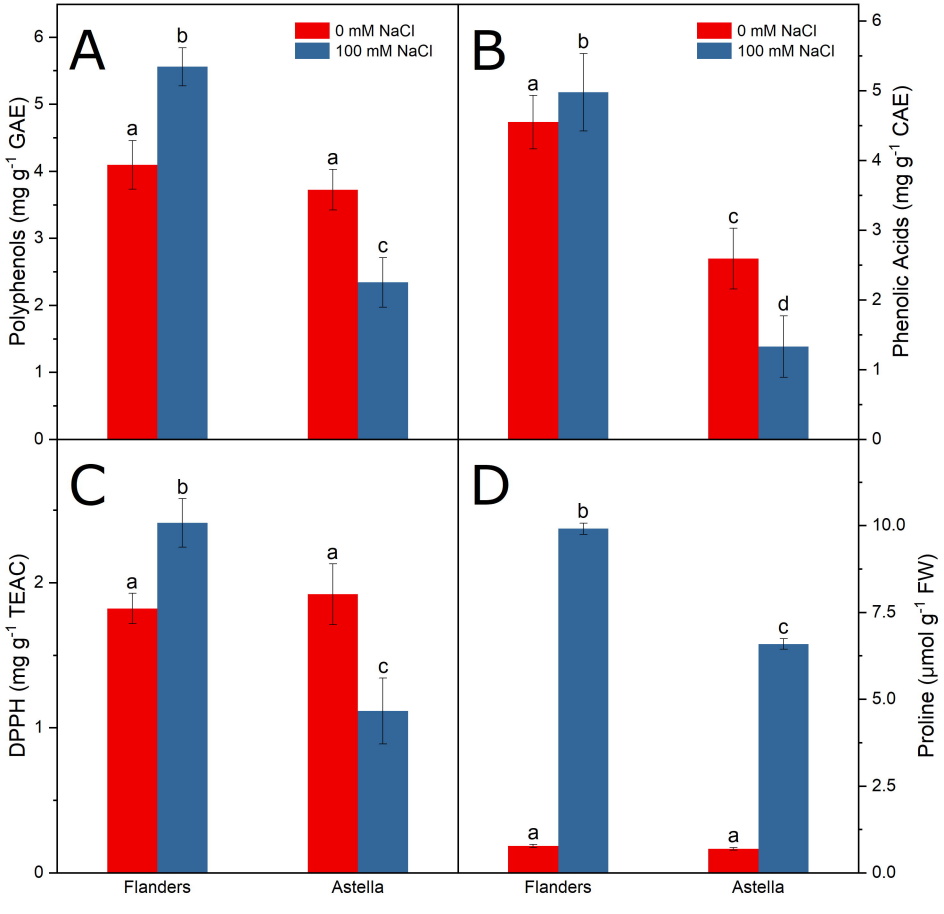

Fig. 4. The estimation of non-enzymatic antioxidants, total radical scavenging activity, and proline content in two flax varieties Flanders and Astella after one week of 100 mM NaCl stress. The non-enzymatic antioxidants polyphenols (A) and phenolic acids (B) are excellent antioxidants due to the presence of multiple hydroxyl groups. (C) The total radical scavenging activity was measured using DPPH assay. (D) Proline provides cellular protection against salt stress in multiple ways. Data represent mean ± standard errors (n = 3) of three biological and three technical replicates. Different letters represent statistical differences at $p < 0.05$ (one-way ANOVA with DMRT post hoc test).

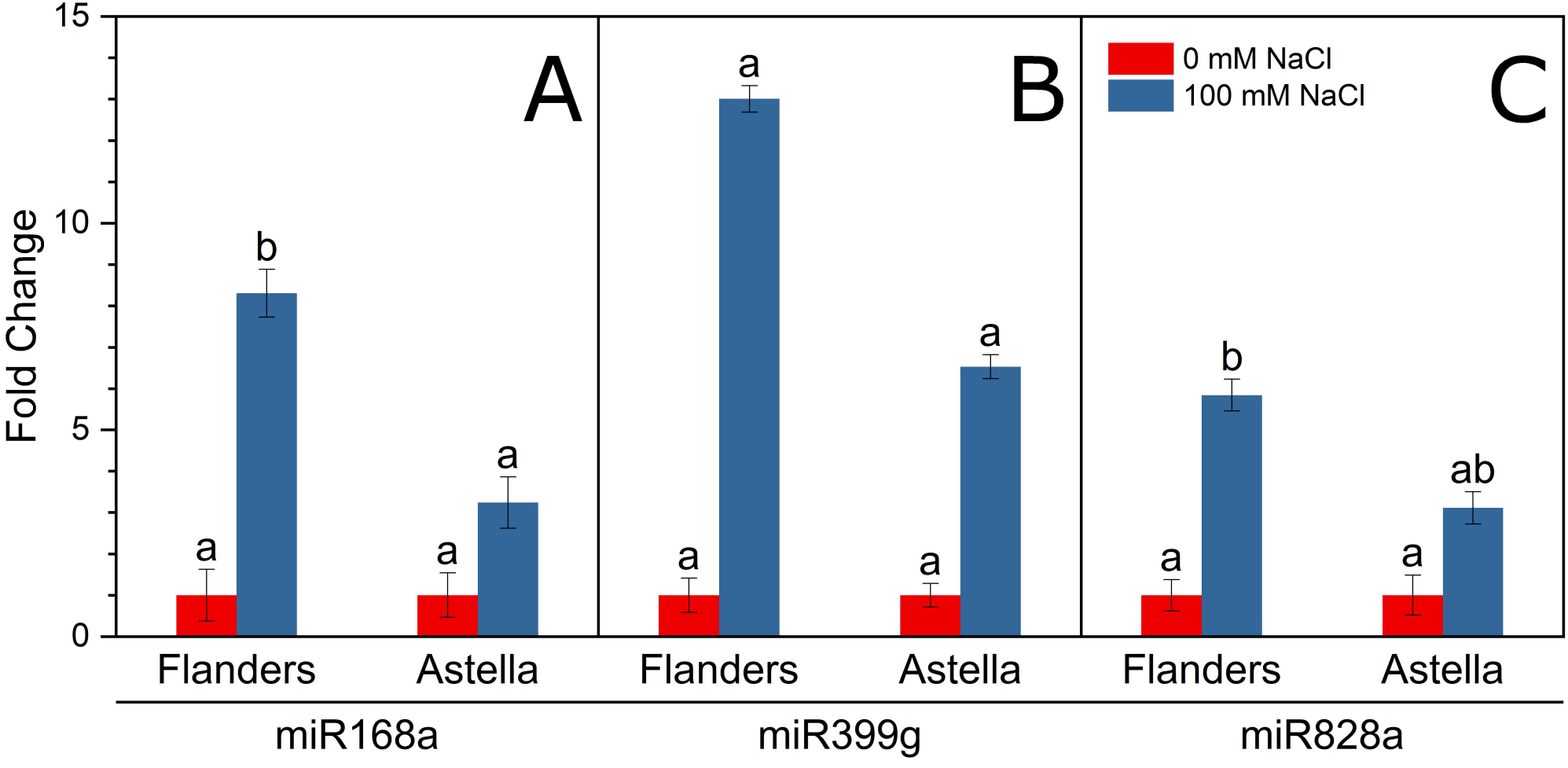

Fig. 5. The expression of lignan-miRNAs in two flax varieties Flanders and Astella after one week of 100 mM NaCl stress. The mRNAs were isolated from treatment plants and the relative expressions of miR168a (A), miR399g (B), and miR828a (C) were measured using the two-tailed qPCR assay kit using Cyklophilin and ETIF5A as internal controls for normalisation. Data represent mean ± standard errors (n = 3) of three biological and three technical replicates. Different letters represent statistical differences at $p < 0.05$ (one-way ANOVA with DMRT post hoc test).

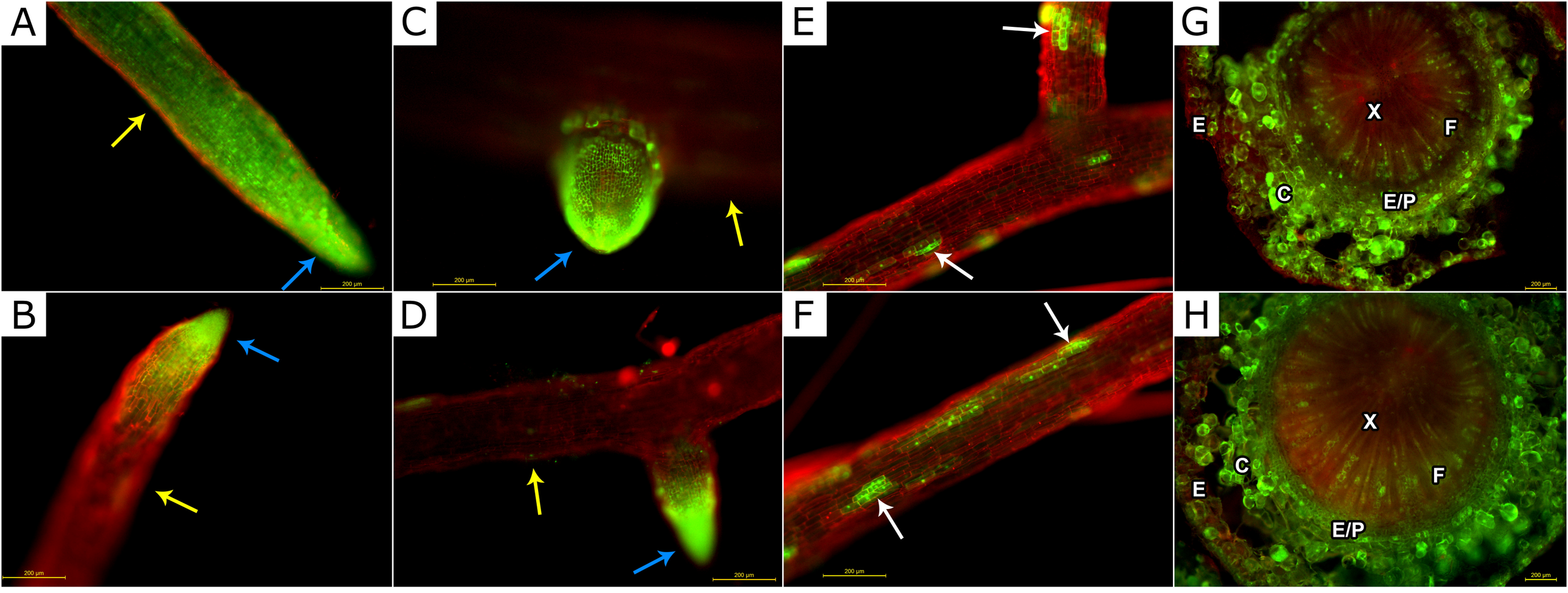

Fig. 6. Fluorescence microscopic study of root cell viability of flax varieties Flanders and Astella using FDA-PI differential staining after one week of 100 mM NaCl stress. Alive cells were green and dead cells were red. (A), (C), (E), and (G) are Flanders roots. (B), (D), (F), and (H) are Astella roots. Root tips (blue arrows in figures (A) and (B)) and lateral root buds (blue arrows in figures (C) and (D)) were alive in both genotypes. The root epidermal layer was mostly dead (yellow arrows in figures (A), (B), (C), and (D)). A sporadic pattern of live cells was found in the root maturation zone (white arrows in figures (E) and (F)). Cross-sectional views also depicted the dead epidermal layer (E in figures (G) and (H)). E epidermis, C cortex, E/P endodermis/pericycle, X xylem, F phloem.

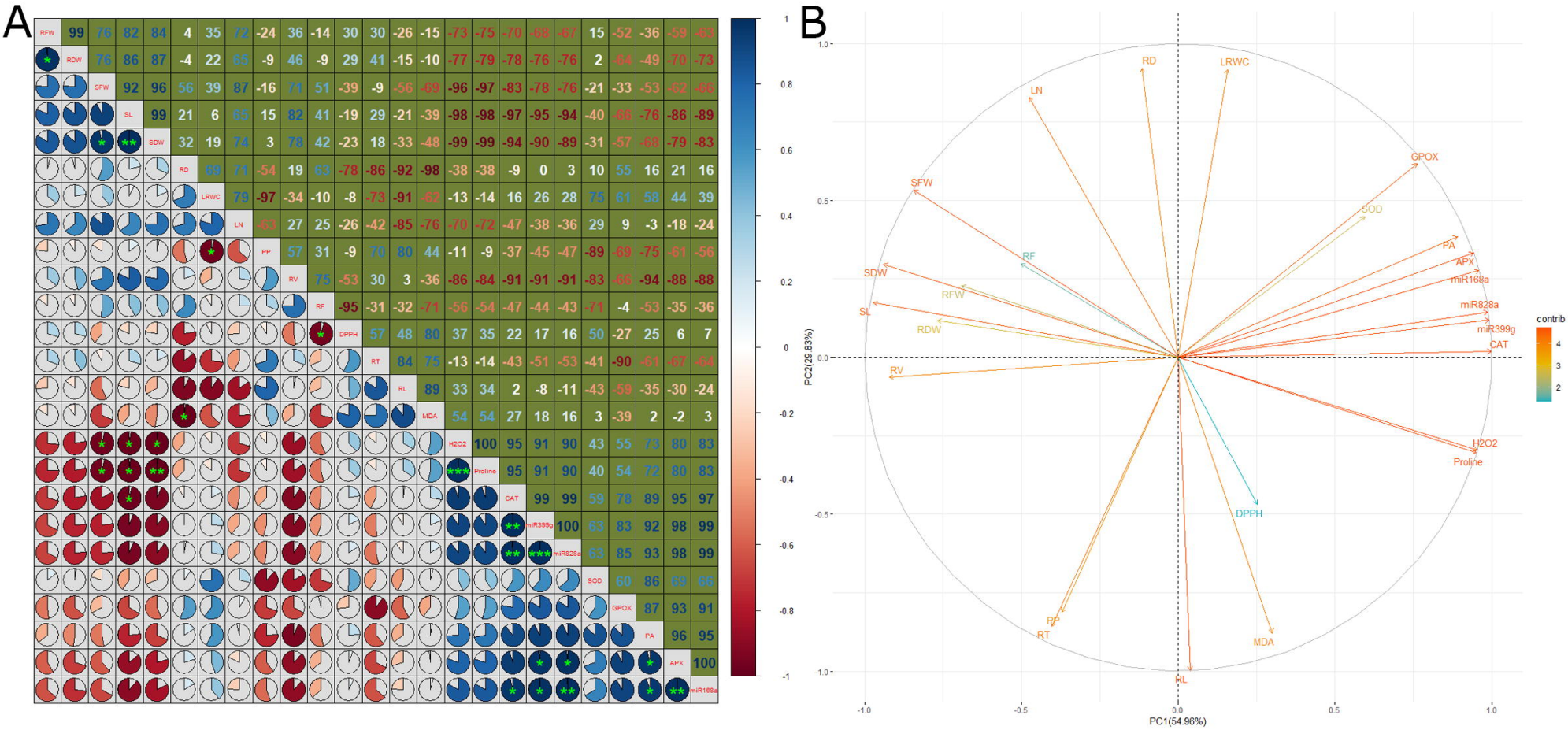

Fig. 7. Correlation analyses using Pearson's correlation (PCC) analysis and principal component analysis (PCA) of the experimental results obtained after providing 100 mM NaCl stress for one week on two flax varieties Flanders and Astella. (A) PCC analysis. We represented the correlation constants as pie figures and the percentage of the correlation values as numbers in the plot. (B) PCA plot represents the loading values of different variables measured in this study. PC1 and PC2 described a total of 84.79% variation.

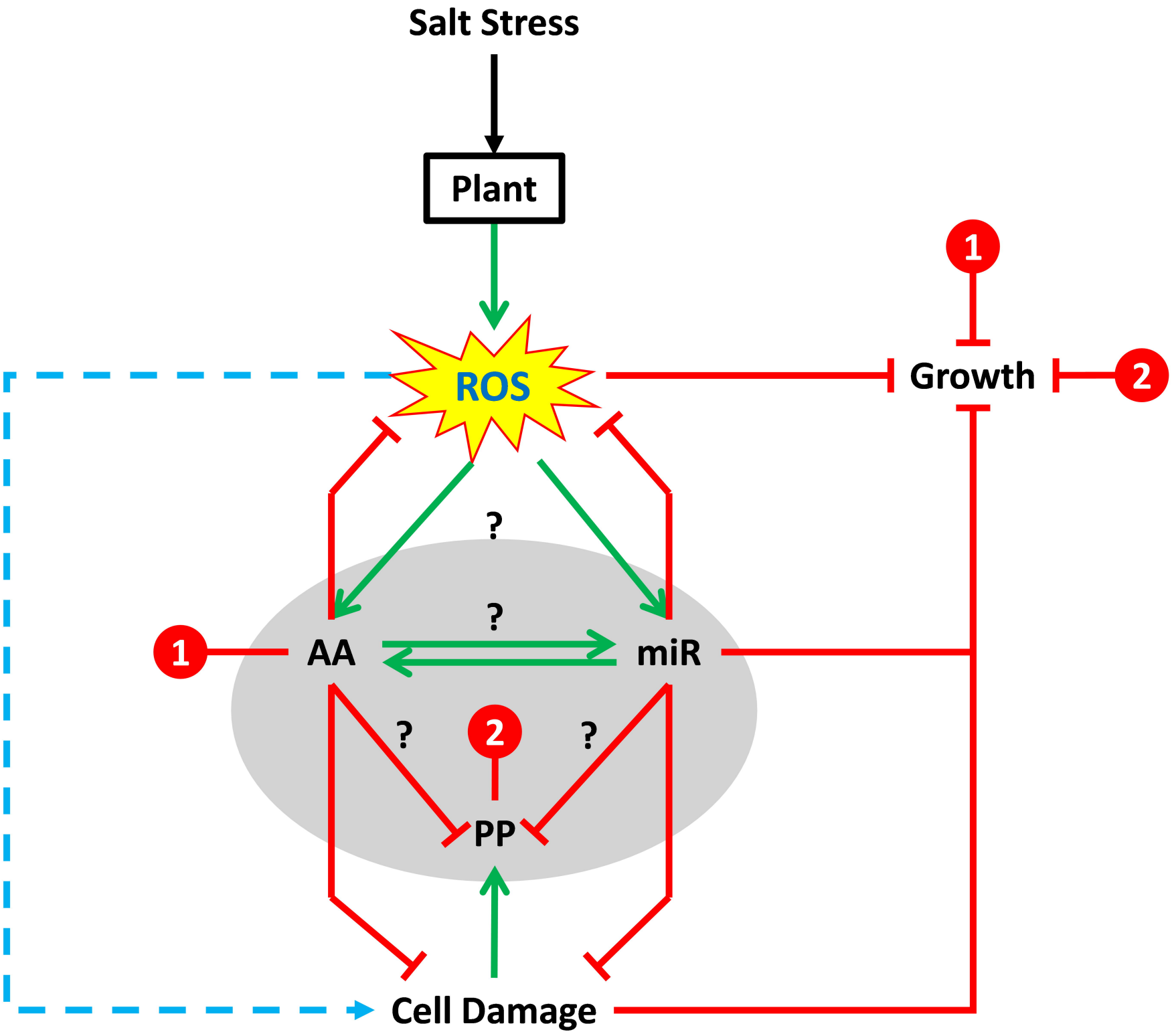

Fig. 8. A speculative representation of flax salt stress mitigation strategy, based on the evidences found in this study. In flax, salt stress-induced ROS can upregulate antioxidants (AA) except polyphenols (PP) and the expression of lignan-related miRNAs (miR). A homeostasis may exist between AA, miR, and PP where AA and miR can upregulate each other, and both can downregulate PP. The grey oval shape highlights the homeostatic relationship. AA and miR can downregulate both ROS and cell damage. ROS promotes cell damage. However, ROS-mediated cell damage remains moderate due to the joint inhibition effect of AA and miR. Plant growth is inhibited by four factors: ROS, AA, miR, and cell damage. AA and PP are connected with growth via the numbers 1 and 2, respectively, written in the red circles. Upregulations and downregulations are represented by solid green and red lines, respectively. The dashed green line represents moderate upregulation. Question marks (?) represent speculative regions.